NASA Tech Briefs

National Aeronautics and
Space Administration

Electronic Components and Circuits

Electronic Systems

Physical Sciences

Materials

Computer Programs

Mechanics

Machinery

Fabrication Technology

Mathematics and Information Sciences

Life Sciences

INTRODUCTION

Tech Briefs are short announcements of innovations originating from research and development activities of the National Aeronautics and Space Administration. They emphasize information considered likely to be transferable across industrial, regional, or disciplinary lines and are issued to encourage commercial application.

Availability of NASA Tech Briefs and TSPs

Requests for individual Tech Briefs or for Technical Support Packages (TSPs) announced herein should be addressed to

National Technology Transfer Center
Telephone No. **(800) 678-6882** or via World Wide Web at **www2.nttc.edu/leads/**

Please reference the control numbers appearing at the end of each Tech Brief. Information on NASA's Commercial Technology Team, its documents, and services is also available at the same facility or on the World Wide Web at **www.nctn.hq.nasa.gov**.

Commercial Technology Offices and Patent Counsels are located at NASA field centers to provide technology-transfer access to industrial users. Inquiries can be made by contacting NASA field centers and program offices listed below.

NASA Field Centers and Program Offices

Ames Research Center
Carolina Blake
(650) 604-1754 or
cblake@mail.arc.nasa.gov

Dryden Flight Research Center
Jenny Baer-Riedhart
(661) 276-3689 or
jenny.baer-riedhart@dfrc.nasa.gov

Goddard Space Flight Center
George Alcorn
(301) 286-5810 or
galcorn@gsfc.nasa.gov

Jet Propulsion Laboratory
Merle McKenzie
(818) 354-2577 or
merle.mckenzie@jpl.nasa.gov

Johnson Space Center
Charlene E. Gilbert
(281) 483-3809 or
commercialization@jsc.nasa.gov

John F. Kennedy Space Center
Jim Alberti
(321) 867-6224 or
Jim.Alberti-1@ksc.nasa.gov

Langley Research Center
Sam Morello
(757) 864-6005 or
s.a.morello@larc.nasa.gov

Glenn Research Center
Larry Viterna
(216) 433-3484 or
cto@grc.nasa.gov

George C. Marshall Space Flight Center
Vernotto C. McMillan
(256) 544-2615 or
vernotto.mcmillan@msfc.nasa.gov

John C. Stennis Space Center
Kirk Sharp
(228) 688-1929 or
technology@ssc.nasa.gov

NASA Program Offices
At NASA Headquarters there are seven major program offices that develop and oversee technology projects of potential interest to industry:

Carl Ray
Small Business Innovation Research Program (SBIR) & Small Business Technology Transfer Program (STTR)
(202) 358-4652 or
cray@mail.hq.nasa.gov

Dr. Robert Norwood
Office of Commercial Technology (Code RW)
(202) 358-2320 or
rnorwood@mail.hq.nasa.gov

John Mankins
Office of Space Flight (Code MP)
(202) 358-4659 or
jmankins@mail.hq.nasa.gov

Terry Hertz
Office of Aero-Space Technology (Code RS)
(202) 358-4636 or
thertz@mail.hq.nasa.gov

Glen Mucklow
Office of Space Sciences (Code SM)
(202) 358-2235 or
gmucklow@mail.hq.nasa.gov

Roger Crouch
Office of Microgravity Science Applications (Code U)
(202) 358-0689 or
rcrouch@hq.nasa.gov

Granville Paules
Office of Mission to Planet Earth (Code Y)
(202) 358-0706 or
gpaules@mtpe.hq.nasa.gov

BLANK PAGE

National Aeronautics and Space Administration

TechBriefs

October 2002
02-10

Electronic Systems

Hardware, Techniques, and Processes

Intuitive Control System for a Dexterous Robot

The operator and robot acting together can respond with nearly natural, humanlike motions.

Lyndon B. Johnson Space Center, Houston, Texas

The Full Immersion Telepresence Testbed (FITT) is an experimental anthropomorphic-robot remote-control system that is so named because it gives a human control operator some of the sensations of the remote environment as though the operator were in that environment in place of the robot. In comparison with older telerobotic control systems, the FITT provides robotic sensory feedback better suited to the operator's senses and enables the operator and robot acting together to respond, with more nearly natural, humanlike motions, to changes in the remote environment. In particular, correlating the operator's movements (principally of the head, arms, and hands) with movements of the robot creates a more intuitive method of teleoperating robotic manipulators. Moreover, the use of an operator's own movements to control the robot provides the operator with useful kinesthetic feedback. The FITT and other systems like it are expected to reduce training time and costs, task-completion times, and operator workloads and errors. Because the FITT concept mates human intelligence with the durability of robots, it is potentially useful for performing complex tasks in harsh environments; for example, cleaning up radioactive and toxic wastes.

An Operator Using the FITT controls a remote robot by a combination of hand, arm, head, and foot motions and vocal commands.

The main component of the FITT is an operator's chair mounted on a rotating base (see figure). By use of foot pedals on the chair, the operator can command direct-drive motors on both the base of the chair and the remote robot. The chair also houses equipment for controlling a video camera unit, manipulators, and end effectors on the remote robot. The operator wears a helmet-mounted video display unit that presents, to the operator, 60°-field-of-view stereoscopic images from the video camera unit on the robot. Stereoscopic imaging creates a perception of depth — one of the most important "immersion" features of the system. The helmet also includes stereophonic headphones for audio feedback and a microphone for operator voice commands. A position-and-orientation sensor on the top of the helmet is the source of commands that control the orientation of the video-camera unit on the remote robot. Other sensors attached to the operator's wrists provide three-dimensional position and pitch, yaw, and roll signals for remote control of positions and orientations of tools held by the robotic manipulators. Instrumented gloves measure the operator's finger-joint angles and the pitch and yaw of the operator's hand, thereby providing signals for dexterous teleoperation of robotic grippers and hands.

Inasmuch as the operator's hands and eyes are "immersed" in the locally synthesized version of the remote environment, they are not available for initiating commands. Therefore, a voice-recognition subsystem provides a convenient way to blend automated commands with direct operator control. To prevent the voice-recognition subsystem from picking up extraneous inputs, the system is set up so that the operator must press a foot pedal to enable the subsystem to receive a spoken command. Once the pedal is released, the command is processed and played back to the operator over a voice synthesizer for confirmation. Motions that can be commanded vocally can vary in complexity from a simple repositioning of a robot arm to a more complex maneuver like grappling and turning a dial.

The software that controls the system is hosted on a UNIX/VersaModule Eurocard (VME) computer workstation and a personal computer with a '486 microprocessor and a voice-recognition circuit board. Data from the position and orientation sensors, instrumented gloves, and foot pedals are sampled at a rate of approximately 10 Hz. The data are sent out over a local-area network, using high-level communication software that enables transfer of data through a C-language program, making low-level driver interfaces transparent.

This work was done by Larry C. H. Li of **Johnson Space Center** *and Myron A. Diftler and Susan S. Shelton of Lockheed Martin. No further documentation is available.*
MSC-22733

FQPSK With an Outer Code for Greater Efficiency

Coding gains are expected, even for reduced-complexity receivers.

NASA's Jet Propulsion Laboratory, Pasadena, California

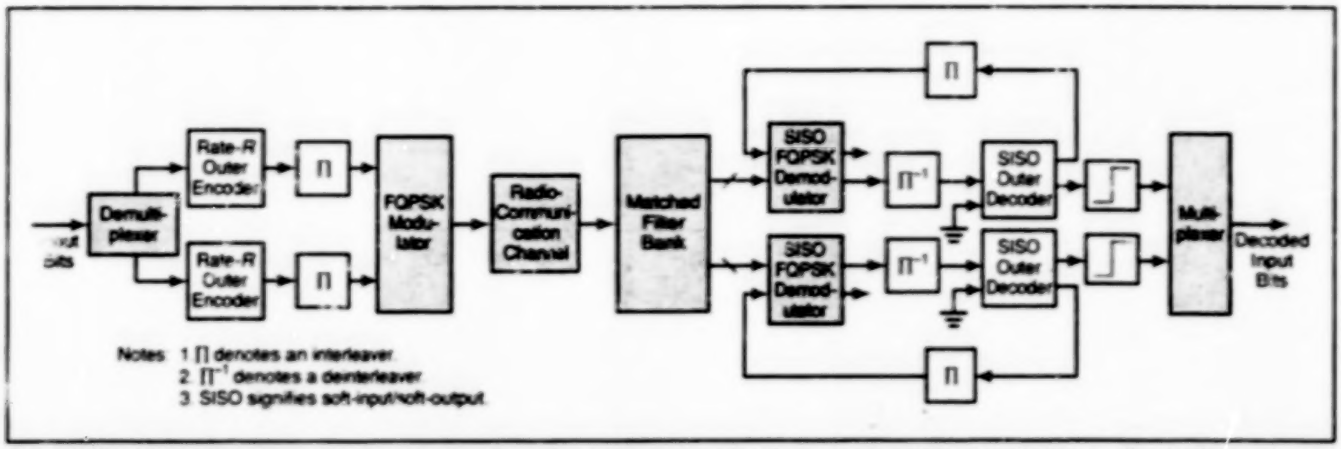

This FQPSK Coding/Modulation and Demodulation/Decoding scheme has been shown, in computational simulations, to offer significant gain over FQPSK modulation and demodulation without coding.

A proposed method of FQPSK modulation and demodulation of a radio signal would incorporate any of a number of relatively simple (short-constraint-length) outer codes. By affording significant coding gains even when using a reduced-complexity (and thus suboptimal) FQPSK receiver, this method would offer the concomitant potential to enhance efficiency in power and spectral width of an FQPSK communication system.

The term "FQPSK" denotes Feher-patented quadrature-phase-shift keying, which is a bandwidth-efficient phase modulation scheme named after its inventor. Among the notable features of FQPSK is shaping of what would otherwise be square in-phase (I) and quadrature (Q) pulse waveforms, such that the signal envelope (in effect, the power of the transmitted signal) remains nearly constant. The shaping involves, among other things, a cross-correlation between the I and Q channels. The nature of the cross-correlation is such as to effectively incorporate a trellis coding scheme into FQPSK.

According to the proposed method, a short-constraint-length code (in effect, an outer code) would be introduced into a data stream via an interleaver prior to modulation of the carrier signal in an FQPSK transmitter. The combination of this outer code with the trellis or convolutional code inherent in FQPSK (in effect, an inner code) would form a concatenated coding arrangement which allows for iterative decoding. At the receiver, the iterative decoding would be part of the demodulation process.

The figure depicts one of a number of generic coding/decoding schemes, admitted by this method, that includes the use of a reduced-complexity receiver. Computational simulations for this scheme with various outer codes, interleaver block sizes, and numbers of decoding iterations demonstrated the potential to obtain coding gains (in terms of signal-to-noise ratio needed to keep the bit-error rate below a specified value) ranging from 3.75 to 7.7 dB.

This work was done by Marvin Simon and Dariush Divsalar of Caltech for **NASA's Jet Propulsion Laboratory**. *Further information is contained in a TSP [see page 1].*

In accordance with Public Law 96-517, the contractor has elected to retain title to this invention. Inquiries concerning rights for its commercial use should be addressed to

Intellectual Property group
JPL
Mail Stop 202-233
4800 Oak Grove Drive
Pasadena, CA 91109
(818) 354-2240

Refer to NPO-30135, volume and number of this NASA Tech Briefs issue, and the page number.

Noncontact Scanning Surface Profilometers

Position-sensitive detectors are used to measure relative surface heights.

John F. Kennedy Space Center, Florida

A class of optoelectronic noncontact computer-controlled scanning surface profilometers is undergoing development for use in automated or semiautomated inspection of nominally flat surfaces. When fully developed, these profilometers would generate three-dimensional maps of the scanned surfaces for characterization of such defects as pits and scratches.

A profilometer of this type includes a two-dimensional (*x*,*y*) horizontal-translation stage, on which the object to be inspected is mounted with the surface of interest facing upward toward a stationary optical head. The optical head contains a laser diode aimed to project a beam of light downward at an angle (22-1/2° in the prototype profilometer) to the perpendicular to the surface of interest. The height of the optical head is set at a nominal vertical distance (0.25 in. (6.35 mm) in the prototype) above the surface of interest. When the vertical distance between the optical head and the surface equals this nominal distance, the spot of light formed on the surface by the laser beam is at a nominal central horizontal position. When the surface lies at a

different height, the spot of light is formed at a different horizontal position.

The optical head contains optics that focus the light reflected from the laser-illuminated spot to a corresponding spot on a one-dimensional position-sensitive detector (PSD), which is a photodetector with electrodes at opposite ends of a line. The deviation of the position of the spot of light along this line from a nominal central position depends on the deviation of the illuminated spot on the surface of interest from the nominal vertical distance below the optical head. The spot of light focused onto the PSD gives rise to photocurrents in the two electrodes; the relative values of these photocurrents depend on the position of the spot of light along the line between the electrodes and thus indicate the local deviation of the height of the surface of interest.

Under computer control, the translation stage is actuated to scan the optical head across the surface. For each increment of horizontal position (x,y), the optical head generates photocurrents indicative of the local deviation of the surface from the nominal vertical distance. The computer builds up a three-dimensional map of the surface from the ensemble of vertical-deviation data for all increments of horizontal position.

The prototype profilometer has been tested in scans of several objects, including a shiny new dime and specimens of diffusely reflective materials. The results of the tests suggest that surface deviations could be routinely resolved to within 10^{-4} in. (5 μm).

This work was done by Jeffrey A. Hooker and Stephen M. Simmons formerly of I-NET for **Kennedy Space Center**.

NASA has granted Laser Technology, Inc., an exclusive license for this technology. Inquiries concerning the commercial use of the "Noncontact Scanning Surface Profilometers" should be addressed to:

John Newman, President
Laser Technology, Inc.
1055 W. Germantown Pike
Norristown, PA 19403
Tel. No.: (610) 631-5043

KSC-11759

Ultrasonic System Tracks Body Movements in Three Dimensions

This system affords centimeter accuracy and overcomes major disadvantages of prior systems.

Lyndon B. Johnson Space Center, Houston, Texas

A system based on ultrasonic sensors has been developed as a means of tracking moving objects with centimeter accuracy. The system is intended especially for tracking pertinent parts of the body of a human subject engaged in control of a remote anthropomorphic robot or immersed in a virtual environment. The system could also be used to track a mobile robot.

There are increasing demands for more sophisticated methods of characterizing the motions of human subjects for the aforementioned purposes. Prior motion-tracking systems have been fairly crude, costly, and tailored for such highly specialized applications as tracking movements of the head or of the eyes only. Whole-body-tracking systems now on the market utilize, variously, expensive optical sensors or magnetic sensors that are susceptible to errors in the presence of nearby metallic objects. To achieve realistic virtual reality, it will be necessary to measure complete body motions by use of systems that are acceptable to human subjects, that interfere minimally with the subjects' motions, and that resist environmental interference. The present system satisfies these requirements.

The present system includes several stationary receiving ultrasonic transducers positioned about the region within which the human subject moves. One or more transmitting ultrasonic transducers are positioned on the parts of the human subject's body that are to be tracked. Putting the transmitters on the human subject minimizes the weight that the subject must carry; the equipment that processes the ultrasonic-signal information is stationary because all such processing is performed in the receivers and in a stationary motion-measurement unit (MMU).

Each transmitter emits a phase-coded waveform at the inaudible frequency of 40 kHz. The outputs of the receivers are sent to the MMU, which performs correlation processing analogous to that performed on microwave signals in the highly successful Global Positioning System. The outputs of the correlation processor are the receiver/transmitter distances; the three-dimensional coordinates of the transmitters are computed from these distances and the known positions of the receivers. No synchronization is needed to enable the receivers and the MMU to distinguish among the signals received from different transmitters because each transmitter uses a unique phase code orthogonal to the phase codes of all the other transmitters.

This work was done by Robert E. Bozek of Genisys Research & Development, Inc., for **Johnson Space Center**. *Further information is contained in a TSP (see page 1).*

MSC-23028

BLANK PAGE

Physical Sciences

Hardware, Techniques, and Processes

BLANK PAGE

Adjusting Polarization To Reduce Error in an Interferometer

There is no need for additional equipment, signals, or signal processing.

NASA's Jet Propulsion Laboratory, Pasadena, California

An unconventional and highly effective technique has been devised to reduce cyclic errors that arise in the operation of a displacement-measuring heterodyne optical interferometer. The cyclic errors are attributable largely to undesired small exchanges of power between light beams that are nominally in mutually orthogonal polarization states (such exchanges are denoted generally as polarization leakage). Unlike some prior techniques for reducing cyclic errors, the present technique does not require additional optical or electronic signals, additional signal processing, or use of optical components other than those of the interferometer itself. Optionally, the present technique can be used in conjunction with the prior techniques to reduce errors further.

The figure schematically depicts a heterodyne optical interferometer that includes a target retroreflector and a fiducial retroreflector, the purpose of the interferometer being to measure displacements between these two retroreflectors. The beam from a single laser is split into two that are shifted in frequency by different amounts. Beam 1, having frequency ν_1, is designated the target beam; beam 2, having frequency ν_2, is designated the local or reference beam. The beams are collimated and then polarized orthogonally to each other: beam 1 is given s (out-of-plane) polarization, while beam 2 is given p (in-plane) polarization. The beams are combined at the injection polarizing beam splitter. A small fraction of the power of both beams is picked off at the reference beam splitter, combined at the reference polarizer, and mixed by the reference photodetector, which generates the reference heterodyne signal at the beat frequency $\nu_1-\nu_2$.

Most of the light propagates to the main polarizing beam splitter. Beam 2 (the p-polarized reference beam) passes through the beam splitter to the signal photodiode. Beam 1 (the s-polarized target beam) is reflected by the beam splitter onto the target path, where it makes a round trip between the target and fiducial retroreflectors and is then reflected into the signal photodiode, wherein beams 1 and 2 are mixed to obtain the target heterodyne signal at the beat frequency. Nominally, the phase of the target heterodyne signal relative to that of the reference signal varies linearly by 2π radians per half wavelength of the target/retroreflector displacement. Hence, the variation of this phase is measured to determine the displacement.

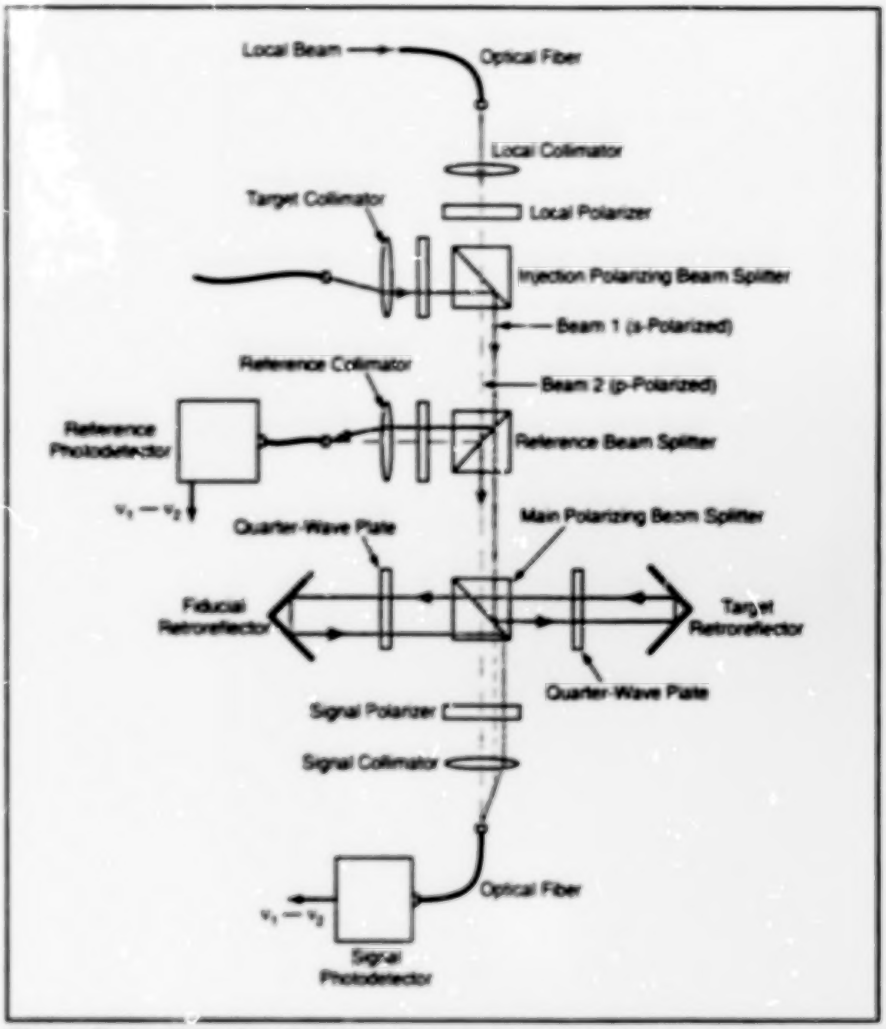

This Is a Typical Heterodyne Optical Interferometer for measuring displacement. Cyclic errors in displacement measurements can be reduced through optimal adjustment of the beam splitters and polarizers to minimize the net deleterious effect of polarization leakage.

In practice, the variation of phase with displacement deviates from perfect linearity because of a number of leakages, which give rise to the aforementioned cyclic errors. The main leakage is the passage of a small portion (≈0.1 percent) of s-polarized power from beam 1 directly through the main polarizing beam splitter to the signal photodetector.

In the present technique, one makes no attempt to reduce this main s-polarized leakage, because it cannot be stopped without also blocking the desired signal. Instead, one takes advantage of the fact that for complex reasons that involve the amplitude and phase relationships among the various polarization components, it is possible to compensate for the effects of the s-polarized leakage by deliberately introducing some additional p-polarized leakage from beam 2 onto the target path. First, one refines the alignments of all relevant optical components to minimize leakages other than the main one. Then, in a multistep procedure, one iteratively adjusts the polarizers and quarter-wave plates to introduce the correct amount of compensatory p-polarized leakage. The procedure can be alternatively characterized as one of seeking the optimum adjustment of the optical components. When optimum adjustment is achieved, the cyclic displacement-measurement error caused by the main and other leakages can be reduced by a large factor (≈10), without nulling the desired signal.

This work was done by Oliver Lay of Caltech for **NASA's Jet Propulsion Laboratory**. *Further information is contained in a TSP [see page 1].*

NPO-30380

Aircraft Anti-Icing Heaters Made From Expanded Graphite

These heaters could be lightweight and inexpensive enough to be practical for small aircraft.

John H. Glenn Research Center, Cleveland, Ohio

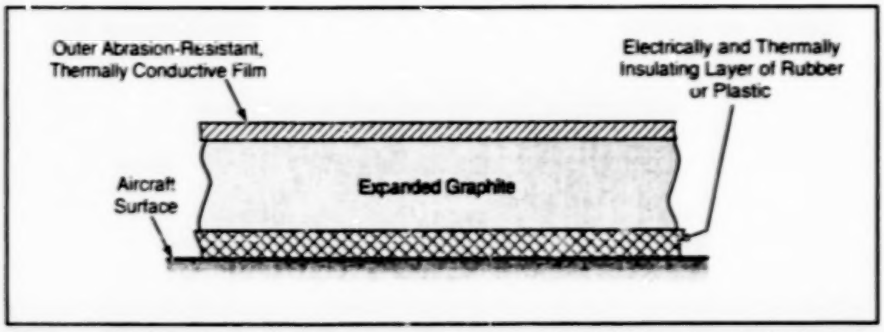

Figure 1. A **Foil of Expanded Graphite** is laminated between an insulating inner layer and a thermally conductive, protective outer layer to form a heater tape that can be bonded to an aircraft surface.

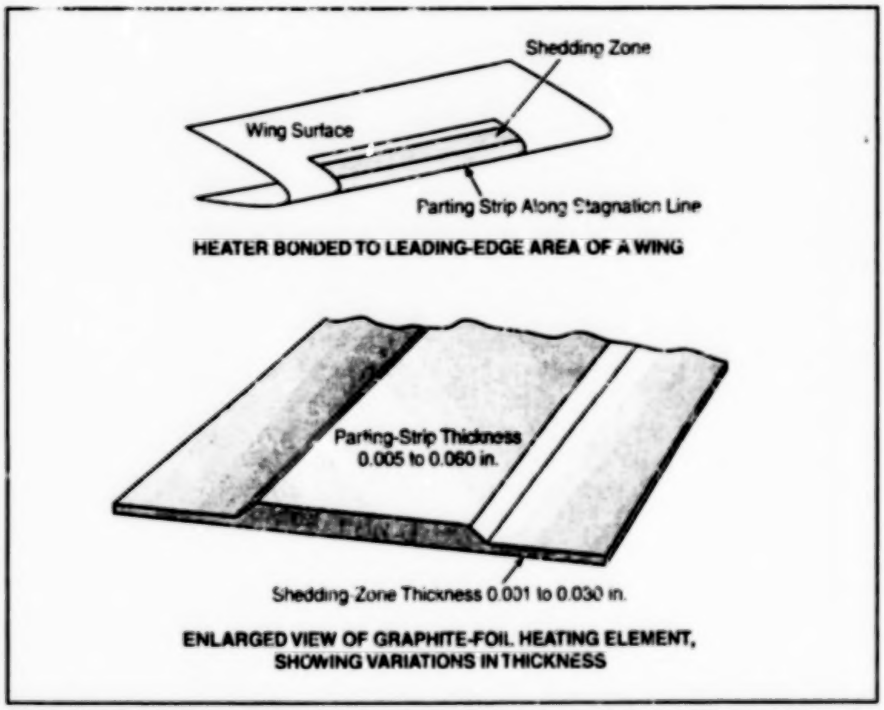

Figure 2. A **Three-Zone Heater** for the leading edge of a wing contains a single electrical-resistance heating element made of expanded-graphite foil with zone-to-zone variations of thickness.

Improved electrical resistance heaters for preventing the accumulation of ice on aircraft surfaces are undergoing development. The primary intended market for these heaters is that of small single- and twin-engine airplanes and helicopters, most of which have not been equipped with anti-icing heaters because the weights and costs of such heaters have made them impractical. The improved heaters are expected to add very little to the weights of aircraft and, when mass-produced, to cost about half as much as do anti-icing systems of prior design. The aircraft could be equipped with high-output alternators to supply the additional electric power needed for the heaters.

In the previously developed electrical anti-icing heaters used on larger aircraft, the resistance heating elements are metallic. Power densities are zoned by use of multiple elements and multiple electrical terminations. A concomitant of multiple heating zones is cold spots and the consequent need for complex control mechanisms: most such systems include multiple timers.

In the present developmental systems, the heating elements are made of expanded-graphite foil, which is flexible, has an electrical resistivity between 6×10^{-4} and 10×10^{-4} Ω-cm, has a thermal conductivity approaching that of brass, and is available in a variety of thicknesses. Typically, the foil in a heater of this type is laminated between (1) an insulating rubber or plastic sheet in contact with an aircraft surface and (2) an outer thermally conductive and protective layer of polyurethane or polyamide with a thickness between 0.001 in. (≈0.03 mm) and 0.010 in. (≈0.25 mm). The heater laminate can be formed as a monolithic tape (see Figure 1) that can readily be bonded to an aircraft surface area where protection against icing is needed.

The heater laminate/tape for a given area need have no more than two electrical contacts, and there is no need for complex controllers for zoning; instead, the spatial variations of power density needed for most effective shedding of ice can be obtained through spatial variations of sheet electrical resistance effected by use of different thicknesses and/or different densities of expanded-graphite foil. For example, one preferred design calls for a heater laid out along the leading-edge area of a wing (see Figure 2). The heater would contain a single foil heating element comprising (1) a central parting strip of greater thickness along the stagnation line wherein the power density would be high enough to keep the temperature above freezing and (2) shedding zones on both sides (downstream) of the parting strip where the thickness of the graphite foil and power density would be lower by an amount that would make the power density at least 3 to 5 times lower than in the parting strip.

Icing-wind-tunnel tests have demonstrated the efficacy of the parting-strip/shedding-zone concept. Icing-wind-tunnel tests have also shown that in comparison with metallic anti-icing heaters, experimental expanded graphite foil heaters are 3 to 5 times more efficient.

This work was done by Robert Rutherford of EGC Enterprises, Inc., for **Glenn Research Center**. *Further information is contained in a TSP [see page 1].*

Inquiries concerning rights for the commercial use of this invention should be addressed to NASA Glenn Research Center, Commercial Technology Office, Attn: Steve Fedor, Mail Stop 4–8, 21000 Brookpark Road, Cleveland, Ohio 44135. Refer to LEW-16895.

Self-Aligning Fiber Couplers for Microsphere Resonators

Critical relative positions would be maintained through contact of precisely dimensioned features.

NASA's Jet Propulsion Laboratory, Pasadena, California

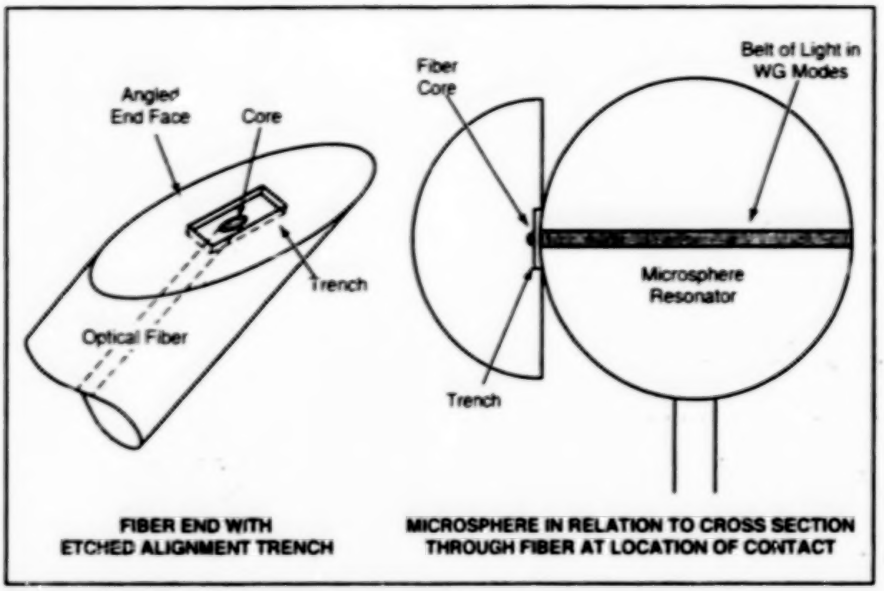

Figure 1. The Trench on the Angled End Face of the optical fiber would be placed in contact with the sphere, astride the belt of light of the WG modes. The depth and width of the trench would establish the desired gap between the fiber core and the sphere.

Fiber-optic couplers for spherical, toroidal, and other, similarly shaped microscopic optical resonators that operate in whispering-gallery (WG) modes would be fabricated with integral alignment features, according to a proposal. These alignment features would facilitate coupling adjustments, which, heretofore, have been difficult and complex, as explained below.

Microsphere and similar resonators have been described in several previous *NASA Tech Briefs* articles. The couplers in question were described in "Simple Fiber-Optic Coupling for Microsphere Resonators" (NPO-20619), *NASA Tech Briefs*, May 2001. To recapitulate: In the WG modes of a transparent microsphere, light orbits inside the sphere, where it is confined by total internal reflection. The high degree of confinement results in high Q (where Q is the resonance quality factor). Light is coupled into or out of the microsphere by exploiting the overlap of (1) the evanescent field of the WG modes with (2) the evanescent field just outside an angled end face of a singe-mode optical fiber.

For efficient transfer of energy, it is necessary to align the microsphere with the fiber such that they are in the correct relative position and orientation for optimum overlap of their evanescent fields:

- The intersection of the core of the optical fiber with the angled end face of the fiber must lie at the point of closest approach of the fiber to the sphere;
- The axis of the fiber must lie in the plane of symmetry of the a circumferential "belt of light" into which the WG modes are concentrated; and
- The gap between the sphere and the angled end face of the fiber must be maintained stable within the range of the evanescent fields — typically between 0.5 and 1.5 μm.

It should be apparent that coupling adjustment between the microsphere and the angled end face of the optical fiber is critical and difficult. Heretofore, it has been necessary to rely on bulky external mounts and translation mechanisms to establish and maintain the correct alignment. The proposed alignment features would ensure the mechanical stability of the gap while reducing the number of adjustment degrees of freedom from five to two, thereby reducing the difficulty of the coupling adjustment and the amount of bulky equipment needed.

The simplest integral alignment feature according to the proposal would be a trench etched into the angled end face of the optical fiber, coincident with the major axis of the face and centered on the end face of the fiber core (see Figure 1). The sphere would be brought into mechanical contact with the long rims of the trench. In this configuration, the depth and width of the trench would determine the size of the evanescent-field coupling gap between the sphere and the end face of the fiber. The contact between the rims and the sphere would not appreciably affect the performance of the microsphere as a resonator because the trench would be made wide enough that the points of contact would lie outside the belt of light.

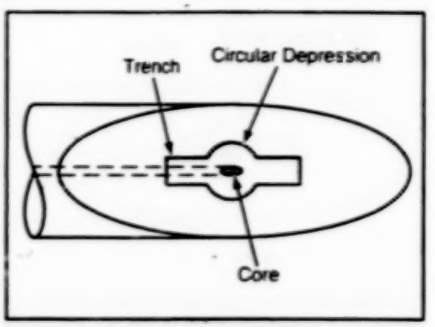

Figure 2. A Circular Depression of depth and width chosen to establish the desired gap could be superimposed on a narrower trench. The circular depression would make it unnecessary to perform an along-the-trench adjustment to place the end of the fiber core at the point of closest approach to the sphere.

To eliminate the need for an adjustment along the trench, one could replace the trench with a circular depression centered on the fiber core. As in the case of a trench, the depth and diameter of this depression would be chosen to obtain the desired gap size. Alternatively, as depicted in Figure 2, such a circular depression could be superimposed on a narrower trench.

This work was done by Vladimir Ilchenko of Caltech for **NASA's Jet Propulsion Laboratory**. *Further information is contained in a TSP [see page 1].*

In accordance with Public Law 96-517, the contractor has elected to retain title to this invention. Inquiries concerning rights for its commercial use should be addressed to

Intellectual Assets Office
JPL
Mail Stop 202-233
4800 Oak Grove Drive
Pasadena, CA 91109
(818) 354-2240
E-mail: ipgroup@jpl.nasa.gov

Refer to NPO-30254, volume and number of this NASA Tech Briefs *issue, and the page number.*

General-Purpose Stereo Imaging Velocimetry

This method enables three-dimensional quantitative characterization of flow fields.

John H. Glenn Research Center, Cleveland, Ohio

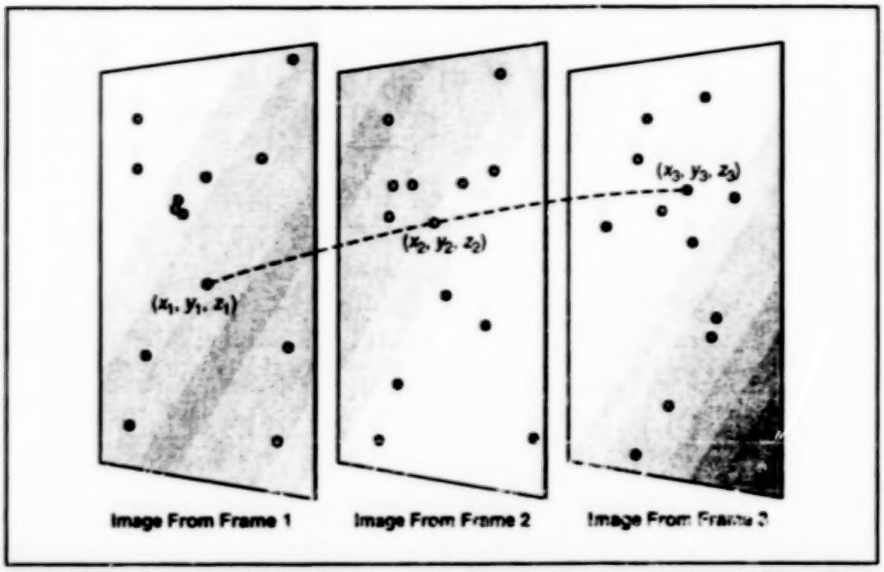

Three-Dimensional Particle Tracking is a major element of the present improved SIV method.

An improved and expanded method of stereo imaging velocimetry (SIV) for diagnosing three-dimensional flows of gases, liquids, and other fluids involves the use of standard charge-coupled-device cameras positioned orthogonally to each other. In addition to providing a full-field, quantitative, three-dimensional map of any optically transparent flow seeded with tracer particles, this SIV method incorporates a camera-calibration technique, in which rotation and translation of camera lenses and optical distortion generated in the lenses are taken into account by use of an accurate two-dimensional-to-three-dimensional mapping function.

Other improvements over the basic SIV method incorporated into the present method include the following:

- An additional image-reconstruction technique accounts for severe distortion in order to enable the reconstruction of incomplete calibration images so that there is less loss of the field of view than there would be in the absence of this technique.
- A new technique for extracting images of tracer particles involves nonattenuating subtraction of image background coupled with a nonattenuating threshold alternative that yields a significant improvement over previous techniques.
- Previously, particles were tracked in two dimensions in each view and then the tracks were matched to produce approximate three-dimensional vectors. A new technique for tracking particles in three dimensions provides true three-dimensional velocity vectors from two orthogonal views or from any set of three-dimensional data. This is a significant advancement in SIV.
- Color image processing has been added, making it possible to analyze flows of multiphase fluids, thereby expanding capabilities and applications beyond those of SIV as practiced heretofore.

While there is a patent on SIV (U.S. Patent 5,905,568), the present method goes beyond the patent, making possible experiments that were previously impossible. In particular, true three-dimensional particle tracking has not been done in SIV until now. The present method makes it possible to perform quantitative, three-dimensional, full-field analyses of flow fields in any fluids that can be seeded with tracer particles.

This work was done by Mark McDowell of **Glenn Research Center**. *Further information is contained in a TSP [see page 1].*

Inquiries concerning rights for the commercial use of this invention should be addressed to NASA Glenn Research Center, Commercial Technology Office, Attn: Steve Fedor, Mail Stop 4–8, 21000 Brookpark Road, Cleveland, Ohio 44135. Refer to LEW-17241.

Improved Capacitive Quality Meter for a Two-Phase Fluid

Features include a better electrode configuration and several hardware improvements.

John F. Kennedy Space Center, Florida

A previously developed quality/flow meter has been redesigned to improve its performance as a device for measuring the quality (but not the flow) of two-phase (liquid + vapor) oxygen or nitrogen flowing in a pipe. As used in engineering disciplines concerned with two-phase flows, "quality" denotes, loosely, volume fractions of liquid or gas. Like some other quality meters, the previously developed meter and the present meter are based on a capacitance-measurement concept: The fluid flows through a space between electrodes, the capacitance between the electrodes is measured, and the volume fractions of liquid and gas are estimated from the effective permittivity, using the known relationships (a) between the effective permittivity and the capacitance and (b) between the volume fractions and the effective permittivity. The estimate of quality can be refined by use of additional data from pressure and temperature sensors.

The previously developed quality/flow meter was described in "Quality/Flowmeter for Two-phase Fluid" (KSC-11725), *NASA Tech Briefs*, July 1997. That instrument was built around a section of pipe that constituted a common outer electrode for two capacitve sensors. The other electrodes for the capacitive sensors were metal rods mounted coaxially within the pipe on electrically insulating radial spacers.

A major difference between the previously developed and present instruments lies in the shapes of the electrodes and the flow cross section. The present instrument contains flat electrodes in a square flow cross section (see figure). In comparison with the previous configuration of concentric round electrodes in a round flow cross section, the present configuration should afford greater accuracy in the measurement of quality because the sensing electric field generated

by flat electrodes is more nearly uniform across the flow path.

The design of the present instrument also incorporates a number of hardware improvements to minimize leakage, provide a rugged connection between an electrical-feedthrough pin and the central plate electrode, position the feedthrough to minimize condensation, and facilitate assembly and disassembly. In addition, the design ensures compatibility of the instrument with liquid oxygen: for this purpose, all parts in contact with liquid oxygen are made of either stainless steel, poly(tetrafluoroethylene) or (in the feedthrough) ceramic.

The technique used to measure the capacitance is somewhat complicated but offers more stability and accuracy than do simpler techniques. First, a circuit that includes timer integrated circuits is used to convert a change in capacitance to a change in the duration of a digital pulse. The duration is then measured by use of an oscillator and a counting circuit. These circuits yield a 12-bit digital counting signal, which is fed to a digital-to-analog converter to generate an analog signal indicative of the measured capacitance and thus the quality. The circuit parameters are chosen so that if, for example, the fluid is a mixture of liquid and gaseous nitrogen, the analog output potential ranges from ≈1 V when only vapor is present to ≈4 V when only liquid is present. The circuitry is capable of sampling the capacitance about 2,000 times per second, but the speed of response is limited by the 0.03-second time constant of a filter in an operational amplifier that process the output of the digital-to-analog converter. This time constant is acceptably short in the original intended application of the quality meter.

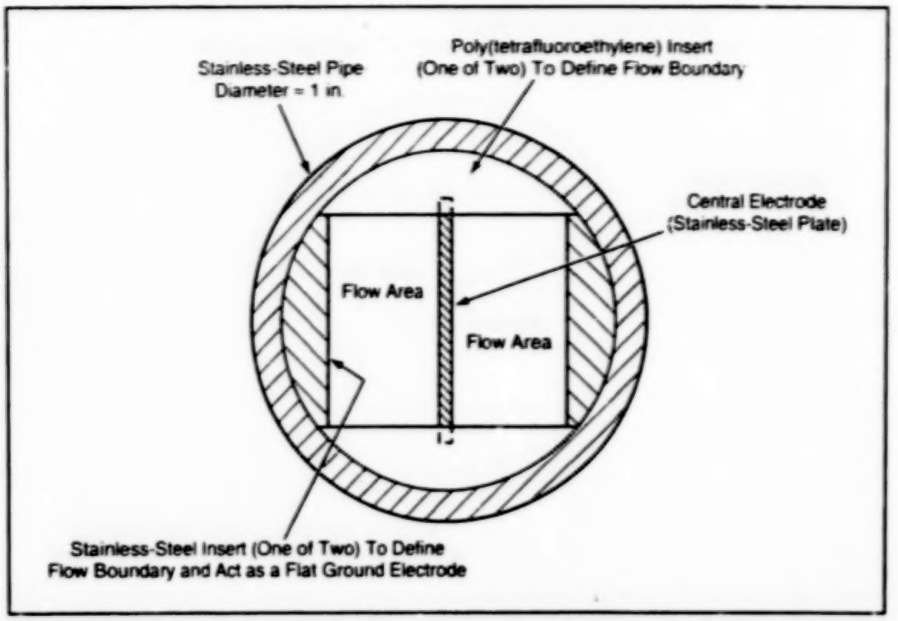

Flat Electrodes give rise to a nearly uniform sensing electric field across the flow area. While the electric field becomes highly nonuniform in the regions above and below the flow area, the poly(tetrafluoroethylene) inserts keep the fluid out of those regions.

This work was done by Rudy J. Werlink of Langley Research Center and Robert C. Youngquist, Robert B. Cox, and William D. Haskell of Dynacs Engineering Co., Inc., for **Kennedy Space Center**. *For further information, please contact Lynne Henkiel at Tel. No. (321) 867-8130 or via e-mail at Lynne.Henkiel-1@ksc.nasa.gov.*
KSC-12080/09

Electrohydrodynamic Conduction Pumps

Pumping is achieved without moving parts and without direct charge injection.

John H. Glenn Research Center, Cleveland, Ohio

Electrohydrodynamic (EHD) conduction pumps have been investigated in theoretical and experimental studies. In general, EHD pumps contain no moving parts. They generate pressure gradients and/or flows in dielectric liquids via any of a variety of interactions between (1) applied electric fields and (2) free and/or bound electric charges in the liquids. Like a related prior device denoted an EHD ion-drag pump, an EHD conduction pump exploits interactions with free charges in liquids, but unlike an ion-drag pump, a conduction pump functions without direct injection of electric charges into the liquid. In the absence of direct injection, EHD conduction pumps are the only EHD devices that can pump isothermal liquids. EHD conduction pumps could be suitable for use as compact, low-power-consumption pumps to enhance flows and thus heat-transfer rates in heat pipes and capillary-pumped loops.

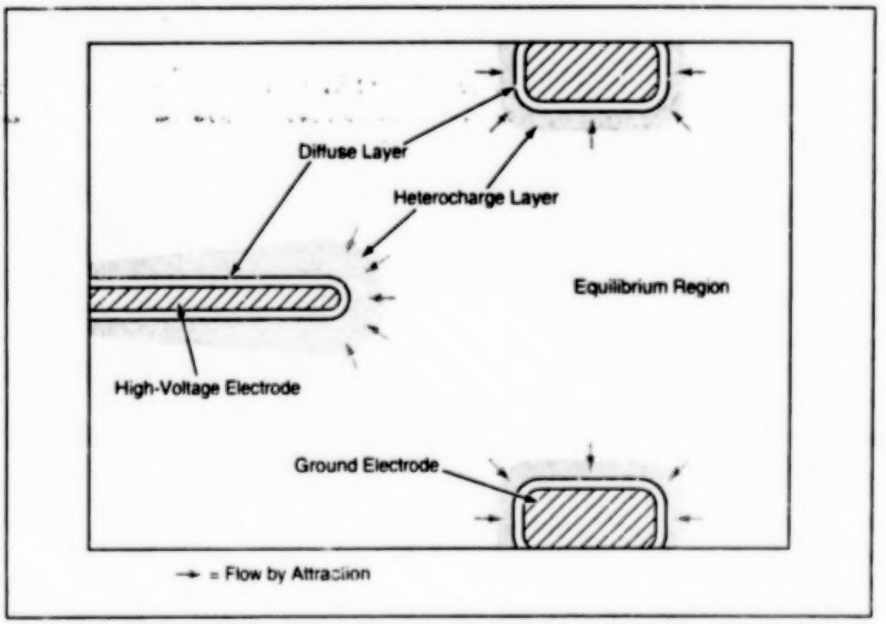

Figure 1. An **EHD Conduction Pump** utilizes free electric charges in heterocharge layers adjacent to electrodes.

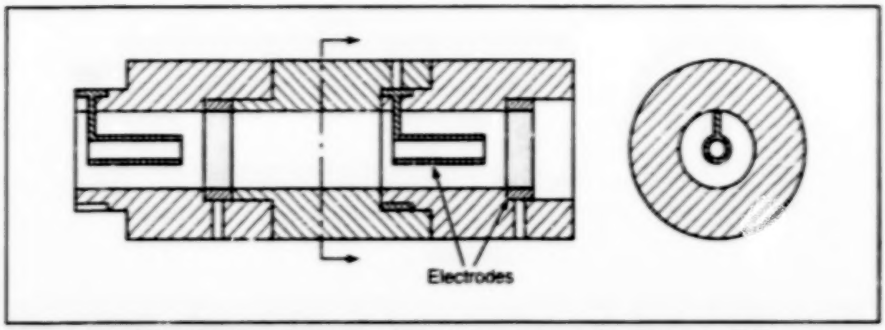

Figure 2. Tube/Ring Electrode Pairs were shown in experiments to be effective for EHD conduction pumping.

In an EHD conduction pump, an electric field is applied to a dielectric liquid through electrodes that are made either flat or else rounded with large curvatures and without sharp points so that there are no electric-field concentrations large enough to give rise to direct injection of charges. Figure 1 depicts salient aspects of the theory of conduction in simplified form. Instead of free charges introduced through direct injection, an EHD conduction pump utilizes free charges in thin heterocharge layers formed in the vicinities of the electrodes through dissociation of molecules within the liquid and recombination of the resulting ions. In order to take advantage of the pumping effect of the heterocharge layers, an EHD pump must also utilize the residual small electrical conduction through the bulk of the otherwise nominally purely dielectric liquid.

Experiments on static-pressure EHD conduction pumps containing three different electrode configurations, using refrigerant 123 (dichlorotrifluoroethane) as the working fluid, have demonstrated the feasibility of this pumping concept. The best performance, observed in the case of a pump containing five hollow-central-electrode/ring-outer-electrode pairs similar to the pair shown in Figure 2, was characterized by a maximum static pressure of 1,034 Pa at an applied potential of 20 kV and a maximum power consumption of 0.57 W.

This work was done by Jamal Seyed-Yagoobi, James E. Bryan, S. I. Jeong, and Y. Fang of Texas A & M University and P. Atten and B. Malraison of LEMD, CNRS (Grenoble, France) for **Glenn Research Center**. *Further information is contained in a TSP [see page 1].*

Inquiries concerning rights for the commercial use of this invention should be addressed to NASA Glenn Research Center, Commercial Technology Office, Attn: Steve Fedor, Mail Stop 7-3, 21000 Brookpark Road, Cleveland, Ohio 44135. Refer LEW-17142.

Relatively Inexpensive Unobscured Large-Aperture Laser-Beam Expander

A design for an unobscured, large-aperture laser-beam expander relies solely on spherical reflecting and refracting surfaces

NASA's Jet Propulsion Laboratory, Pasadena, California

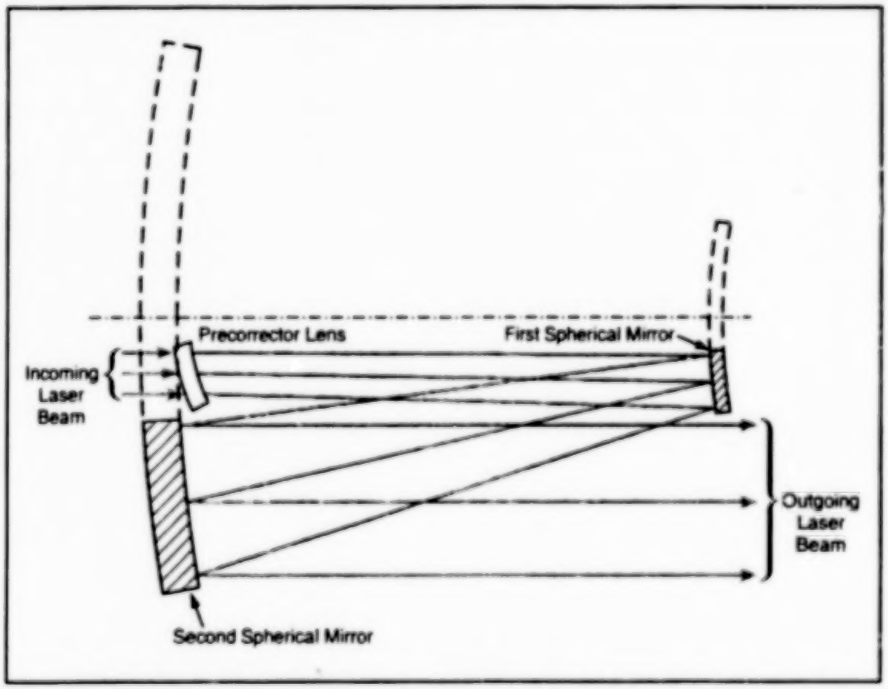

This Laser-Beam Expander, containing only one lens and two mirrors with all spherical optical surfaces, offers good performance at relatively low cost.

A design for an unobscured, large-aperture but otherwise compact laser-beam expander relies solely on spherical reflecting and refracting surfaces, yet provides a reasonably well corrected wavefront suitable for most applications. This design results from a tradeoff among compactness, cost, and performance.

The classical approach to the design of such a laser-beam expander typically involves the use of off-axis, aspherical mirrors and/or large lenses, which are expensive to fabricate. Spherical-surface mirrors and small spherical-surface lenses can be fabricated at substantially lower cost, but a beam-expander design based on such spherical-surface optics involves a tradeoff between compactness and performance.

The approach taken to arrive at the present design starts from an understanding that the design of a laser-beam expander need not afford all the performance characteristics of the classical telescope designs from which most beam-expander designs are derived. One consideration is that a laser-beam expander is not required to perform well over a wide field of view. A second consideration is that a laser-beam expander is required to perform well at only one wavelength. A third consideration is that limitations of fabrication capabilities make it impossible to achieve the maximum theoretical performance of a classical design in real hardware and that, in practice, a beam expander fabricated from a suboptimum design that calls for a small number of spherical (only) surfaces can be made to perform as well if not better, while costing much less.

The foregoing reasoning led to the present design (see figure), which calls for a minimum number of surfaces, all spherical, the largest being mirrors rather than lenses. The first optical element encountered by the

incoming laser beam is a precorrector lens, which is so named because the radii of its spherical surfaces are chosen to introduce spherical aberration equal and opposite to that from the mirrors that follow. The lens is centered in the beam and tilted to introduce the correct amount of aberration to compensate for (precorrect) the off-axis aberrations caused by using the spherical mirrors at non-normal angles of incidence. The precise required thickness of the lens, radii of curvature of its surfaces, and angle at which it is tilted, depend on the index of refraction of the lens material, the wavelength of operation, and the mirror configuration.

The second optical element encountered by the laser beam is the smaller of two spherical mirrors. This mirror is tilted to redirect the now expanding beam so that, once collected and collimated by the larger spherical mirror, the beam passes the smaller spherical mirror without being obscured. The third and final optical element encountered by the laser beam is the larger spherical mirror, which is concave and is tilted to redirect the now collimated and expanded outgoing beam parallel to the incoming (unexpanded) beam. As is often found in optical systems of similar function, the placement and tilt of the mirrors can be described as being off-axis segments of a pair of larger mirrors sharing a common optical axis. The key distinction is that the "off-axis segments" in the design presented here are of spherical mirrors, so are themselves spherical, and hence easier (= relatively inexpensive) to fabricate.

The resulting wavefront performance is exceptionally well-corrected, with a nominal residual error so low as to be negligible in comparison with the effects of fabrication and assembly effects. The only aspect of performance that might be considered adverse is that the beam expansion is slightly anamorphic: the cross section of the output beam is elliptical, the minor axis being between 0.90 and 0.95 times as long as the major axis. If necessary, the anamorphism could be corrected by use of a more complex precorrector lens, still at an overall cost much less than that of a classical beam expander.

This work was done by Jeffrey Oseas of Caltech for **NASA's Jet Propulsion Laboratory**. *Further information is contained in a TSP [see page 1].*

NPO-30432

Spotlight Radiometer

The principal use of this instrument would be remote sensing of gases.

NASA's Jet Propulsion Laboratory, Pasadena, California

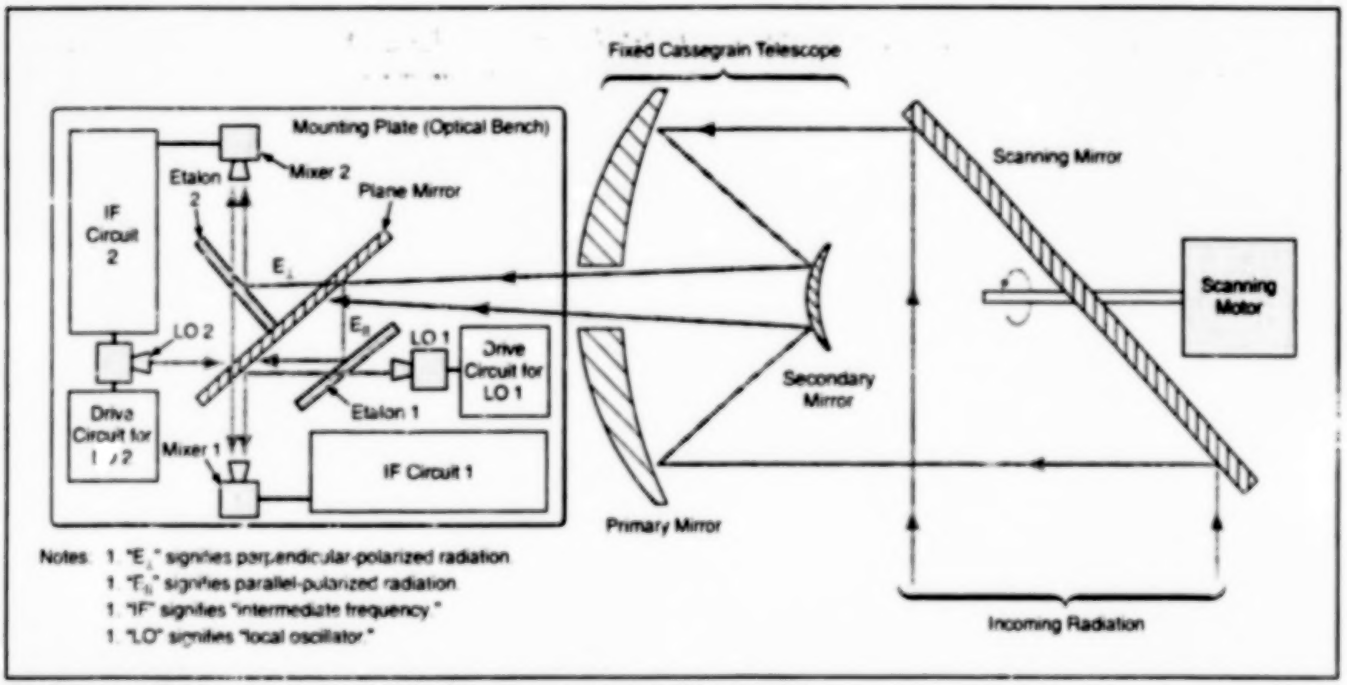

The **Scanning Mirror** and its motor would be the only moving parts in this instrument.

A proposed radiometric instrument denoted the spotlight radiometer (SLR) would operate in a frequency band centered at ≈557 GHz and would scan in a conical or circular pattern. The SLR was conceived for use in obtaining spatially and spectrally resolved indications of CO and H_2O molecules in the Martian atmosphere. The basic SLR design is also adaptable to terrestrial use and to operation in different submillimeter-wavelength bands.

Although the SLR would include a Cassegrain telescope, the telescope would not be moved to effect scanning. Instead, the telescope would be fixed and scanning would be effected by simply turning a lightweight, flat mirror in front of the telescope. The entire instrument would fit inside a cylindrical envelope or canister, the diameter of which need not exceed that of the primary reflector of the telescope. The advantages afforded by the foregoing design features include light weight, convenient placement of the electronic and optical components, and simple, compact construction.

The angle between the flat scanning mirror and the optical axis of the telescope would determine the cone angle of the scan pattern. This angle could be set, for example, to enable scanning of the horizon or of an annular region of the sky. The flat mirror could be constructed easily and, because it could be very lightweight, a low-torque scanning motor would suffice and it would be possible to scan at a high rate. At one or more angular positions of the scan, the viewing of the exterior scene could be blocked out for radiometric calibration.

After reflection from the scanning mirror

and passage through the Cassegrain telescope, incoming radiation would pass through a polarizing beam splitter in the form of a wire grid tilted at an angle of 45° to the optical axis. From this beam splitter, each of the two polarization components of the radiation would travel to one of two heterodyne radiometers. Hence, the SLR would provide simultaneous readings of both perpendicular- and parallel-polarized radiation.

In addition to a local oscillator, each heterodyne radiometer would include a silicon etalon beam combiner. The use of a silicon etalon (in contradistinction to the use of a different device) as a diplexer would simplify the design of the input portion of the radiometer and would provide a temperature-insensitive means of coupling the local-oscillator and incoming radiation into the down-converter portion (submillimeter-wave mixer) of the radiometer. The use of a double-sided mirror coplanar with the polarizing grid would facilitate the positioning of the two radiometers within a confined space. Even if polarization measurements were not required in a given application, the use of both polarization channels would make it possible to increase the signal-to-noise ratio slightly.

The mixer and local oscillator of each heterodyne radiometer would be conveniently situated near their respective drive elements and within the shadow of the primary telescope mirror. All of the electronic and optical components could be mounted on a single plate made of a lightweight material (e.g., a carbon-fiber composite). The rear surface of this plate could be used for heat sinking.

This work was done by Peter Siegel of Caltech for **NASA's Jet Propulsion Laboratory**. *Further information is contained in a TSP [see page 1].*
NPO-30183

Slab-Waveguide Interferometer for Sensing Ammonia in Wet Air

Ammonia changes the pattern of interference between TM_0 and TM_1 waveguide modes.

John H. Glenn Research Center, Cleveland, Ohio

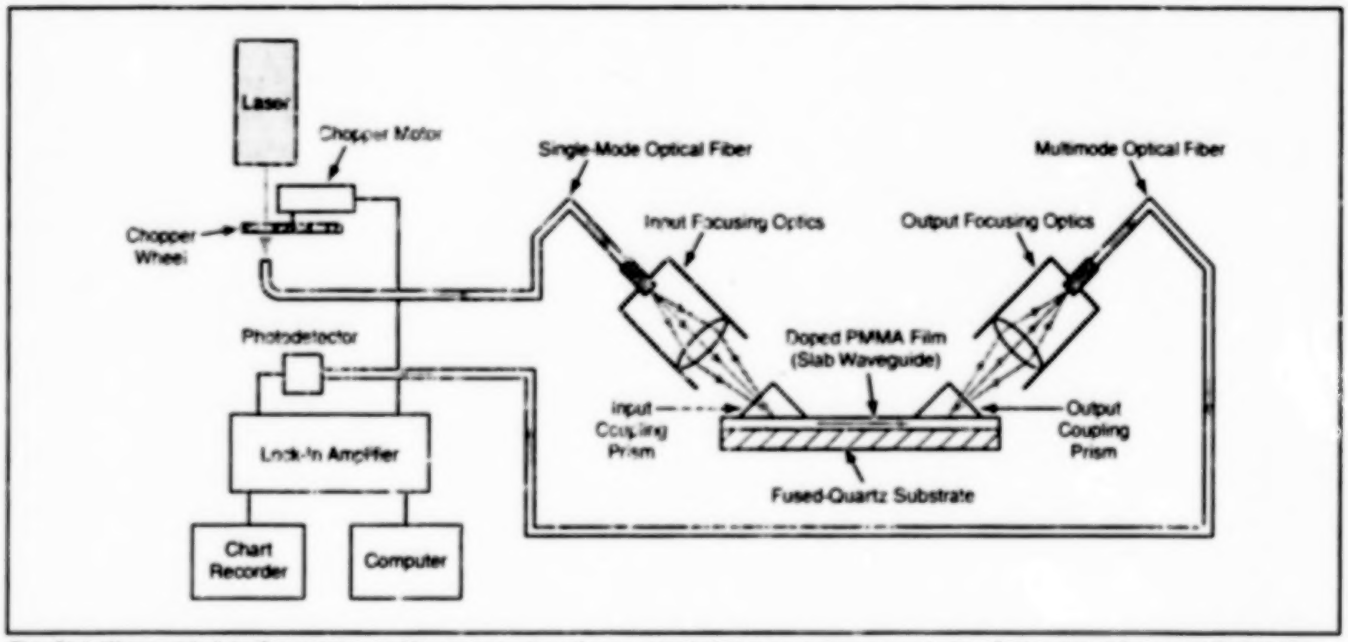

This **Slab-Waveguide Interferometer** provides an indication of the ammonia-induced change in the index of refraction of the doped PMMA film.

The figure depicts a single-arm, slab-waveguide interferometer that has been demonstrated to be useable as a means of sensing ammonia in wet air. The slab-waveguide portion of this device comprises a 2-μm-thick film of poly(methyl methacrylate) [PMMA] on a substrate of fused quartz. The PMMA layer acts as a waveguide because its index of refraction is greater than the indices of refraction of both the fused quartz on one side and the ambient air on the other side. The PMMA film is doped with bromocresol purple — an indicator dye that causes the index of refraction of the film to vary with the amount of ammonia that diffuses into the film from the ambient air. The remaining basic features of design and operation, as described below, are devoted to enhancing and measuring the change in an optical phase difference attributable to the change in the index of refraction and thus to the presence of ammonia.

At opposite ends of the waveguide, the wide rectangular facets of triangular input and output coupling prisms are pressed against the surface of the PMMA film. The prisms are made of gallium gadolinium garnet. Light from a He-Ne laser (wavelength of 633 nm) is chopped and sent through a single-mode optical fiber to input focusing optics. The design of the input focusing optics and the input coupling prism is such that two transverse magnetic (TM) modes — the ones of zeroth and first order (TM_0 and TM_1, respectively) — are excited simultaneously in the slab waveguide. After traveling along the waveguide, the waves propagating in the two modes encounter the output coupling optics, which are similar to the input coupling optics except that their role is to focus light in the two modes onto an end face of a multimode optical fiber. Because the two modes are coherent, they give rise to an interference pattern. With proper design of the optics and proper placement of the multimode optical fiber, the spatial period of the fringes is several times the diameter of the fiber.

The multimode optical fiber leads to a photodetector. The output of the photodetector is processed through a lock-in amplifier synchronized with the chopper. When index of refraction of the doped-PMMA waveguide film changes upon exposure to

wet ambient air containing ammonia, the resulting change in its index of refraction causes a change in the differences between the phases of the TM_0 and TM_1 modes at the output end of the waveguide. This change in phase difference causes the interference fringes to shift with respect to the input face of the multimode optical fiber, thereby further giving rise to a change in the intensity of light arriving at the photodetector. In an experiment, the sensitivity of this device was found to be a phase-difference change of 2π radians (one full oscillation of the intensity of light arriving at the photodetector) per approximately 200 parts per million of ammonia.

The design of this device has not yet been optimized with respect to the laser wavelength, choice of waveguide polymer, and concentration of dopant. In addition, it may be necessary to add a reference interferometer arm isolated from the ambient air to provide temperature compensation, because the single-arm version described above is highly sensitive to temperature (of the order of 2π radians of phase-shift change per 1 °C change in temperature).

This work was done by Sergey Sarkisov of Alabama Agricultural and Mechanical University for **Glenn Research Center**. *Further information is contained in a TSP [see page 1].*

Inquiries concerning rights for the commercial use of this invention should be addressed to NASA Glenn Research Center, Commercial Technology Office, Attn: Steve Fedor, Mail Stop 4–8, 21000 Brookpark Road, Cleveland, Ohio 44135. Refer to LEW-17189.

Infrared Fiber-Optic Endoscope

Thermography could be performed in confined spaces and harsh environments.

Langley Research Center, Hampton, Virginia

A proposed infrared transmitting fiber-optic endoscope, which would partly resemble a visible-light fiber-optic endoscope, instrument could be used to perform thermal imaging in harsh environments and/or confined spaces in a variety of situations in aerospace, industrial, automotive, and medical settings.

Like a typical visible-light fiber-optic endoscope, the proposed instrument would include a coherent fiber-optic infrared bundle with an objective lens attached to its distal end. The lens would focus energy from the scene under observation onto the input face of the fiber-optic bundle. Of course, unlike in a visible-light fiber-optic endoscope, both the lens and the optical fibers would be made of materials that transmit a substantial proportion of the infrared energy in a wavelength range useful for observing at the temperature range of interest.

Another infrared-transmissive lens at the proximal end of the coherent fiber-optic bundle would focus the infrared image of the scene from the output face of bundle onto a planar array of infrared photodetectors. The outputs of the photodetectors would be processed by electronic circuitry to generate a temperature map of the scene and/or a visible analog of the infrared image of the scene. In the processing, the photodetector outputs would be converted to temperatures at corresponding locations in the scene on the basis of a photodetector calibration and radiative properties that may be known or assumed in accordance with physical conditions in the scene.

The main advantage of this instrument is that the relatively compact, rugged viewing optic could be inserted in the confined and/or inhospitable environment containing the scene to be observed, while the rest of the instrument could be accessible and located in a hospitable environment. The instrument would be tailored for the temperature range of interest through the choice of lens and fiber-optic materials as mentioned above plus the choice of photodetectors suitable for the wavelength range corresponding to the temperature range. For example, one could choose a PtSi-based detector array for shorter wavelengths corresponding to higher temperatures or an HgCdTe-based array for longer wavelengths corresponding to lower temperatures.

This work was done by Stephen E. Borg and Christopher E. Glass of **Langley Research Center**. *Further information is contained in a TSP [see page 1].*
LAR-16149

Fiber-Optic Probe Uses Evanescent Waves To Sense Biofilm

Biofouling can be detected in less time than that needed in conventional culture-plate counting.

Lyndon B. Johnson Space Center, Houston, Texas

A compact instrument includes a fiber-optic probe that utilizes the evanescent-wave interaction to measure the accumulation of a biofilm. This instrument is a prototype of instruments that could be used to effect continuous monitoring and provide early warning of biofilms associated with bacterial contamination in diverse water systems, including potable-water supply systems, industrial heat-exchanger systems, and heating and cooling systems for buildings. The instrument makes it possible to detect biofouling of such systems sooner than the ends of the 24-to-48 hour incubation periods needed for conventional detection of bacteria by culture-plate counting.

The instrument has overall dimensions of 4 by 17 by 1.5 in. (about 10 by 43 by 4 cm) and is made from inexpensive optoelectronic components. One of the components is a light-emitting diode (LED). Modulated light from the LED is launched into the fiber-optic probe, which includes an unclad length of optical fiber that serves as a sensory element. Light travels along the fiber, past the sensory element, to a photodetector. The output of the photodetector is processed by a digital-interface circuit board connected to the parallel input port of a computer. In essence, what one seeks to compute is the proportion of light reaching the photodetector as an indication of the amount (if any) of biofouling on the sensory element.

Any biofilm attached to the sensory length of fiber affects the evanescent wave of the light propagating in the fiber. The effect is primarily a result of (1) a change in the index of refraction to which the evanescent wave is subject and (2) increased scattering of light. The evanescent wave is shallow enough that the instrument exhibits a significant response to as little as a monolayer of bacteria.

The design of the instrument was guided by a mathematical model that assisted in the optimization of the instrument performance and the prediction of the response of the instrument to specified changes in the index

of refraction of the medium surrounding the sensory element. The overall response of the instrument to a change in the index of refraction is characterized by, among other things, a time of less than 1 minute. In tests in which bacterial cultures were added to, variously, distilled water or plant-nutrient solutions, peak first-stage responses occurred within 1 to 6 hours and peak second-stage responses took place after 8 to 10 hours.

This work was done by Ron Michaels of Polestar Technologies, Inc., for **Johnson Space Center**.
MSC-22880

Ellipsoidal Collecting Horns for Ultrasonic Leak Detectors

Ellipsoidal reflectors have been proposed as collecting horns for ultrasonic leak detectors. Exploiting the classical focusing characteristics of ellipsoids, these reflectors would facilitate and enhance the detection of leaks in situations in which it is possible to bring leak-detecting sensors to within distances of the order of centimeters from leaks, but not closer. Leak detectors based on this concept could complement commercially available ultrasonic leak detectors equipped with paraboloidal reflectors for focusing over much longer distances. In a typical application, an ultrasonic receiving transducer would be positioned at one of the two foci of an ellipsoidal reflector. At the end opposite the transducer, the reflector would be shielded to provide an opening for the entry of sound and for positioning the reflector near a leak. When the reflector and transducer assembly was positioned to make the leak (or, more generally, any other small source of ultrasound) be at the other focus of the ellipsoid, the maximum amount of radiated ultrasound would be focused onto the transducer, resulting in maximum detector response. The principle of operation has been verified in experiments.

This work was done by Robert C. Youngquist and Robert Cox of Dynacs Engineering Co., Inc. for **Kennedy Space Center**. *Further information is contained in a TSP [see page 1].*
KSC-12082

Regulating Pressure-Volume Control of a Gas Blanketing Liquid R-124

A system for storing and circulating a refrigerant liquid [R-124 (chlorotetrafluoroethane)] includes a reservoir and a subsystem that regulates the pressure of nitrogen gas in the head space of the reservoir. The purpose of the pressurization is to prevent cavitation in a pump that circulates the liquid. It is necessary to keep enough nitrogen in the system to keep the pressure high enough to prevent cavitation even when the liquid is at its coldest and thus at its smallest volume. It is also necessary to satisfy a competing requirement to, when the refrigerant is at its warmest and thus at its greatest volume, prevent the pressure from exceeding the level at which a relief valve opens and vents the head-space gaseous mixture of refrigerant vapor and nitrogen to the atmosphere. The pressure-control subsystem includes a supply of nitrogen at a pressure of 80 psig (gauge pressure of 552 kPa), a commercial electronic pressure regulator, a programmable-logic controller, and pressure and temperature sensors in the reservoir. The pressure-control subsystem adjusts the nitrogen pressure to the optimum value for the sensed temperature, thereby preventing both cavitation and venting.

This work was done by Michael Katz and Charles Walker of United Space Alliance for **Kennedy Space Center**. *Further information is contained in a TSP [see page 1].*
KSC-12167

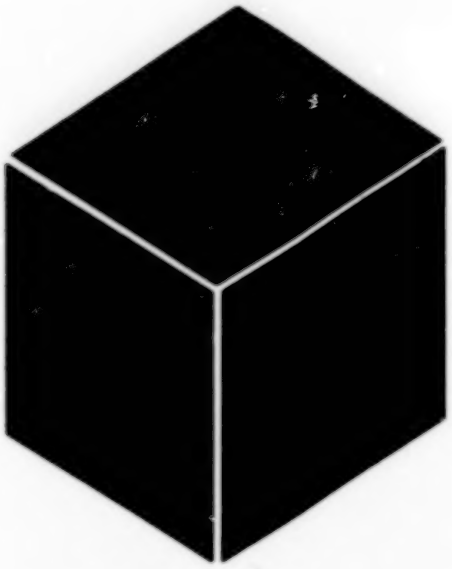

Materials

Hardware, Techniques, and Processes

Books and Reports

BLANK PAGE

Ablative Coat Protects Against Brief, Intense Heating

A substrate can be protected against a rocket blast for a short time.

John F. Kennedy Space Center, Florida

An ablative composite coating has been developed to protect a steel substrate against a short-duration exposure to supersonic stream of hot gases and molten ceramic particles. In the original application, the short-duration hot, abrasive flow is resultant from the shuttle solid-fuel rocket motor exhaust during launch. The steel substrate to be protected is a holddown-post blast shield on a space-shuttle mobile launcher platform. The maximum temperature in the rocket blast exceeds 5,500 °F (≈3,000 °C), and the heat load on the blast shield can exceed 8,000 Btu/ft²s (≈91 MW/m²s). Other components and launch accessories exposed to similar intense, short-duration, heat loads could also be protected by use of similar composite coatings.

The basic architecture of this ablative composite coating is a high-density, room-temperature-cured silicone (RTV), reinforced with layers of glass fabric. By chemically preparing the substrate and fabric laminates and by use of vacuum consolidation during cure, a coating is created that not only provides the known ablative properties of silicone resins, but also provides the physical strength to withstand the enormous pressures and shear forces encountered during exposure with delamination or debonding from the substrate.

In this application, the substrate is prepared by sandblasting an application of a hydrolyzable silicone primer. If necessary, the thick trowelable putty is made from RTV and a ceramic powder. Layers of glass fabric are preprocessed to remove the sizing and chemically treated to ensure a strong resin-to-fiber bond. The laminate is then built up to the required thickness by applying alternating layers of fabric and silicone resin. After sufficient layers have been applied, caul plates are applied and the entire blast cover cured under moderate vacuum pressure to squeeze out excess resin and ensure a strong coating-to-substrate bond.

The figure shows a newly coated blast shield and a blast shield after an exposure to the rocket exhaust. The average thickness of the ablative coating when new was 0.542 in. (≈13.8 mm); the average thickness after exposure was 0.165 in. (≈4.2 mm). The thickness of the coating was found to be adequate everywhere except at two corners. Ceramic particles in the rocket exhaust did not adhere to the silicone rubber. The silicone rubber at the steel substrate and the laminate exhibited no visible signs of deterioration. This observation was interpreted as signifying that the ablative coat succeeded in keeping the temperature at the bond surface below 600 °F (below approximately 320 °C). Except for a minor surface crack at one corner, the blast shield was undamaged.

NEWLY COATED BLAST SHIELD

BLAST SHIELD AFTER EXPOSURE TO ROCKET EXHAUST

Some of the Layers of Fabric and silicone rubber were removed from the laminated coat by exposure to rocket exhaust. However, enough of the laminate remained (except at the corners) to prevent excessive heating of the substrate.

This work was done by Robert C. Dyer, Martin J. Wilson, Jean M. Charvet, and Burton J. Pelkey, Jr., of United Space Alliance for **Kennedy Space Center**.

Further information is contained in a TSP [see page 1].

This invention is owned by NASA, and a patent application has been filed. Inquiries concerning nonexclusive or exclusive license for its commercial development should be addressed to the Technology Programs and Commercialization Office, Kennedy Space Center, (321) 867-8130. Refer to KSC-12285.

Insertion of Reactive Material for Treating Groundwater

There is no need to remove most of the overlying soil.

John F. Kennedy Space Center, Florida

An improved method of inserting reactive material in the ground for treating groundwater contaminated with chlorinated solvents has been devised. An older method involves the removal of a significant portion of soil overlying the treatment volume, and consequently the expensive off-site disposal of the large amount of removed soil (some or all of which is contaminated). In the improved method, only a relatively small amount of soil need be removed.

The first step in the improved method is to remove approximately the first 4 ft (1.2 m) of soil from above the water table where the reactive material is to be placed. Hollow casings are inserted in the ground surface over the treatment site, then hammered down to the required placement depth. (The placement depth in the original application at Kennedy Space Center was 40 ft (12 m).)

Once each casing reaches the required depth, a gravity-fed hopper is used to fill the casing with the reactive material plus, if needed, bulking material to increase permeability. The casing is then removed, leaving behind a column of treatment material. In this manner, several such columns are positioned throughout the treatment volume.

An *in situ* deep-soil-mixing rig is then used to mix the reactive columns with the adjacent soil. Thorough mixing is achieved by up-and-down motion of the rig. The rig includes paddles, the turning of which acts in coordination with the up-and-down motion to help increase the permeability of the soil.

This work was done by Jacqueline Quinn of **Kennedy Space Center** *and Debra R. Reinhart, Christian A. Clausen III, Manoj B. Chopra, and Cherie L. Geiger of the University of Central Florida. Further information is contained in a TSP [see page 1].*

This invention has been patented by NASA (U.S. Patent No. 6,207,114). Inquiries concerning nonexclusive or exclusive license for its commercial development should be addressed to the Technology Programs and Commercialization Office, Kennedy Space Center, (321) 867-4879. Refer to KSC 11957.

Books and Reports

Lightweight Solar Sail for a Spacecraft Flying Near the Sun

A report proposes a high-temperature-resistant solar sail with an areal mass density less than 1 g/m^2, for a spacecraft that would approach the Sun to within a distance of 0.2 astronomical unit (≈3 × 10^7 km). The sail would be made in multiple segments of a carbon microtruss fabric held in a network of tensioned lines. The segments and network would be designed to minimize tension in the fabric. The porosity of the fabric would be tailored so that to photons, the fabric would behave as though it were solid. Reflective metal surface films could be attached to the fabric. In advanced versions, the fabric could be directly coated with metal; or, alternatively, the fabric surface would be the sail surface and there would be no metal layer. The sail fabric would be wrapped around a sail cylinder and deployed by use of centrifugal force. A separate structure next to the sail cylinder would contain most of the "ship cylinder" hardware and would be ejected after deployment of the sail to reduce the mass staying with the sail.

This work was done by Charles Garner, Stephanie Lafer, Timothy Knowles, and William Lewman of Caltech for **NASA's Jet Propulsion Laboratory**. *To obtain a copy of the report, "Solar Sail Design for Interstellar Probe," see TSPs [page 1].*
NPO-20654

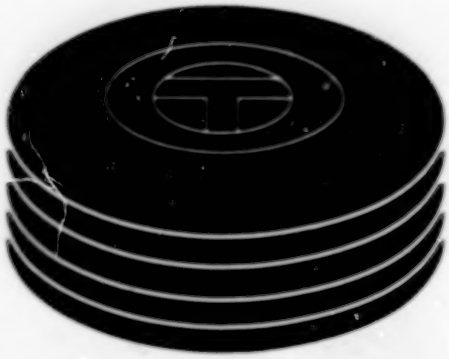

Computer Programs

Physical Sciences

Mathematics and Information Sciences

BLANK PAGE

Physical Sciences

Program Finds Target-Chemical Signals in Multisensor Outputs

A computer program deconvolves the digitized outputs of multiple chemical sensors in an array to extract indications of the identities and concentrations of target chemicals (which could be individual compounds or specified mixtures of compounds). Chemical-sensor arrays — denoted, variously, as electronic noses and electronic tongues — can be used for diverse purposes, including monitoring the quality of air in enclosed spaces, medical diagnosis involving specified chemical compounds or bacteria distinctive of particular diseases or infections, and monitoring the quality of food. The program follows a nonlinear-least-squares approach to the analysis of data from a chemical-sensor array. In experiments, the program was found to be capable of identifying and quantifying both single compounds and mixtures of large numbers of compounds.

This program was written by Hanying Zhou of Caltech for **NASA's Jet Propulsion Laboratory**. *Further information is contained in a TSP [see page 1].*

This software is available for commercial licensing. Please contact Don Hart of the California Institute of Technology at (818) 393-3425. Refer to NPO-30437.

Program Computes Outer-Space Heat-Sink Temperatures

TSCALC is a computer program that calculates the space sink temperature (T_S), defined as the equilibrium temperature of a spacecraft heat-dissipation radiator or other object nominally isolated except for radiative exchange of heat with the Sun, or any star for which equilibrium sink temperatures are to be evaluated; planets, in the neighborhood of which the thermal environment is of interest; and interstellar space. TSCALC utilizes the gray-body Stefan-Boltzmann equation and the equations for radiant fluxes as functions of distances between, and orientations of, bodies engaged in radiative exchange. Factors taken into account by TSCALC include (1) distances from the spacecraft to the Sun and any planets in the neighborhood of which a spacecraft has to operate; (2) angles between the radiator surface and lines of sight to the Sun and a neighboring planet; (3) the ratio between solar absorptivity and thermal emissivity of the radiator surface; (4) the "View Factor to Space," which is a function of the solid angle subtended by interstellar space as viewed from the radiator; (5) the luminosity, L, of the stellar heat source ($L = 3.86 \times 10^{26}$ W for the Sun); and (6) the albedos of planets, in the vicinity of which a spacecraft will operate. The T_S computed by TSCALC can be used, along with the thermophysical properties of the radiator material and the temperature of a spacecraft heat source, as inputs to spacecraft-radiator design code that computes the area of a radiator needed to dissipate a given heat load while operating at a given temperature $>T_S$.

This work was done by Albert J. Juhasz of **Glenn Research Center**. *Further information is contained in a TSP [see page 1].*

Inquiries concerning rights for the commercial use of this invention should be addressed to NASA Glenn Research Center, Commercial Technology Office, Attn: Steve Fedor, Mail Stop 4–8, 21000 Brookpark Road, Cleveland, Ohio 44135. Refer to LEW-16852.

Mathematics and Information Sciences

Program Analyzes Use of Registers by Another Program

Regprof is a computer program that analyzes the use of registers by another program that runs on a PowerPC 750 (or equivalent) computer. Regprof is useful for showing how well compilers make use of registers and for obtaining an indication of the susceptibility of application programs to radiation-induced changes in register bits. Regprof goes through the source code of the program in question, analyzing each instruction to determine what registers it uses and whether the instruction loads a register with a value or uses a value already in a register. A register is marked as being in use between the instruction that loads a value into it and the last instruction in which that value is used. Upon completion of this analysis, a histogram table that shows how many registers are in use at each line of the analyzed program is printed. One limitation of this analysis is that it does not take account of program flow and, instead, is performed as though all lines of the analyzed code were executed in sequence. This is adequate for most compiler code, but in some cases, one might obtain a distorted representation of register usage.

This program was written by Paul Springer of Caltech for **NASA's Jet Propulsion Laboratory**. *Further information is contained in a TSP [see page 1].*

This software is available for commercial licensing. Please contact Don Hart of the California Institute of Technology at (818) 393-3425. Refer to NPO-30347.

Real-Time Desktop Manager

This program manages other programs and displays.

Real-time Desktop Manager (RDM) is a computer program that manages displays and application programs. RDM was developed for use in connection with NASA's remote manipulator system (RMS) group of flight controllers; it could also be used in chemical plants, laboratories, factories, hospitals, and other settings where it is necessary to monitor many data streams. The RDM displays are data-driven, and color is used to indicate the criticality of a display. There are other programs that perform such functions, but they are very expensive and, unlike RDM, do not afford graphical capabilities.

RDM is written in the ANSI-C computing language, using the Motif widget set, for execution in the Unix operating system. The sources of input to RDM are a series of input files, the user, and an information-sharing-protocol (ISP) data-acquisition system, which is maintained as an independent program. RDM enables the user to create a data display with the help of previously stored input files that define a main window display, a menu-bar display, and individual display windows. The displays are driven by data received from an ISP server and input from the user. The program reads input files to create easily configurable displays that can be modified before flights and simulations without having to modify and recertify software.

RDM conforms to the Mission Control Center (MCC) Human and Computer Interface guidelines. It utilizes other software

already in use in the MCC, plus other software that has, variously, been developed or purchased by NASA. Some investigation of other graphical software tools revealed that display windows are created within programs that must be compiled for each change. In RDM, it is not necessary to compile for each change in a display. The user simply modifies the input files and initiates the execution of RDM, that reads the files.

This program was written by Sharon L. Valentine, Charles C. Birkner, and Ronald L. Kerr of Rockwell International Corp. for **Johnson Space Center**.
MSC-22727

Embeddable Fuzzy-Logic-Toolkit Software for Tcl/Tk

Advantages include minimal cost, versatility, and relative simplicity.

A computer program of the fuzzy-logic-toolkit type has been developed as a relatively simple, portable, highly compatible, means of providing fuzzy-logic reasoning capabilities for control and expert-system applications. This program is designed to work with the high-level scripting language Tcl/Tk and to invoke the access-to-data capabilities of an information-sharing protocol (ISP). This program supplies the numerous functions necessary for effective utilization of fuzzy-logic reasoning methods and overcomes many disadvantages of other fuzzy-logic toolkits. The program, written in the C language, is relatively small, portable, efficient, and embeddable. Better yet, this program is flexible in that it includes a source code that can be improved or developed to add further capabilities and features. The most commercially advantageous feature of the program is that it is available essentially without cost. With the help of this program, users can learn how to write fuzzy-logic programs for real applications.

This software is based partly on the FuzzyCLIPS software, which was developed by the National Research Council of Canada by modifying a prior Johnson Space Center software innovation known as CLIPS (for C Language Integrated Production System). FuzzyCLIPS is written in the C language and contains a source code that is freely available to users. In addition, FuzzyCLIPS was also designed to be embeddable in other application programs, making it most suitable for the development of toolkit-type software.

In the development of the present fuzzy-logic-toolkit program, the FuzzyCLIPS source code was combined with an interface code, thereby registering FuzzyCLIPS functions with Tcl commands while at the same time converting data types between the two codes as necessary. In the end, 13 commands were created to provide access to FuzzyCLIPS from within Tcl.

Other programs were then developed as test cases to demonstrate the capabilities of this fuzzy-logic-toolkit program. In one case, a simple shower-control problem, provided with the original FuzzyCLIPS software, was used to exhibit the ability of the toolkit program to incorporate fuzzy logic into a control application program. Another case, more relevant to NASA's needs, the use of fuzzy-logic control with ISP telemetry data was demonstrated. In this demonstration, ISP data were presented to the user with a graphical display created by use of the Tk software. During each cycle of ISP data, a fuzzy-logic control procedure was invoked, and the results of this invocation were displayed. The degrees of membership of input and output data in fuzzy sets were also presented graphically to users.

In both the aforementioned test cases and in use at NASA, the versatility of this fuzzy-logic-toolkit program has been demonstrated. The main benefit that it affords to NASA is an ability to create more "intelligent" flight-control displays. Beyond NASA, this software can be used to create displays that make background use of fuzzy-logic reasoning while at the same time presenting the results of an expert system (e.g., a diagnostic system) in the foreground.

This program was written by John C. Limroth of Rockwell International for **Johnson Space Center**.
MSC-22730

Mechanics

Hardware, Techniques, and Processes

Books and Reports

BLANK PAGE

Formation Alignment of Multiple Autonomous Vehicles

Alignment is achieved by use of lasers, optical sensors, and rule-based controls.

NASA's Jet Propulsion Laboratory, Pasadena, California

A table-top experiment on formation alignment of three air-levitated robotic vehicles has been performed to demonstrate the feasibility of a more general concept of controlling multiple robotic vehicles to make them move in specified positions and orientations with respect to each other. The original intended application of the concept is in the control of multiple spacecraft flying in formation, as described in "Synchronizing Attitudes and Maneuvers of Multiple Spacecraft" (NPO-20569) elsewhere in this issue of *NASA Tech Briefs*. In principle, the concept could also be applied on Earth to control formation flying of aircraft or to coordinate the motions of multiple robots, land vehicles, or ships.

The experimental system is, of course, much simpler than a fully developed multiple-robot formation-alignment system would be. In this system (see figure) the three vehicles are levitated over a flat table by air bearings generated from internal supplies of compressed air. Each vehicle is equipped with valves that can be opened momentarily under electrical control to allow jets of compressed air to escape in order to control horizontal translation of the vehicle and/or rotation of the vehicle about a vertical axis.

The problem chosen for the experimental demonstration is to make the three vehicles position and orient themselves at the corners of an equilateral triangle. Even in this simple system, the formation-alignment scheme is highly complex; the most that can be done to describe it in this article is to do so indirectly by summarizing the major features of the equipment and the formation-alignment scenario as follows:

The formation-alignment scheme chosen to solve the triangle problem involves the use of lasers, optical sensors, and control subsystems that implement rule-based motion-control algorithms in response to optical-sensor readings. The control subsystems of the vehicles also communicate with each other via radio transceivers.

Each vehicle is equipped with a laser and with an optical-sensor module with an optical axis at an angle of 60° with the laser axis. One of the vehicles is designated the leader, while the others are designated follower 1 and follower 2. The leader initiates the alignment process by activating its laser and rotating to look for follower 1. When the optical sensors of follower 1 detect the laser beam from the leader, follower 1 sends a radio signal to the leader to cause the leader to stop rotating. Follower 1 then performs fine adjustments of its attitude relative to the laser beam from the leader.

Once follower 1 has completed its fine alignment, it turns on its laser and sends a radio signal that commands follower 2 to search for the laser beam from follower 1. This search involves a sequence of prescribed rotations and translations. Follower 2 terminates its search as soon as its optical sensors detect the laser beam from follower 1. Follower 2 then performs fine adjustments of its attitude with respect to the laser beam from follower 1.

Once follower 2 has completed its fine alignment with the laser beam from follower 1, follower 2 turns on its laser and begins a final alignment motion in which it translates along the laser beam from follower 1. When an optical sensor on the leader intercepts the laser beam from follower 2, the leader sends a radio signal that tells follower 2 to stop. At this point, alignment is complete.

This scheme causes the three vehicles to lie at the corners of an equilateral triangle, with the laser of each vehicle aimed at an optical sensor on another vehicle. However, in this scheme, no attempt is made to control the size of the triangle; this is because of the difficulty of optically measuring short distances typical of the intervehicular distances in this experimental system.

This work was done by Fred Y. Hadaegh and Kenneth Lau of Caltech and Paul K. C. Wang and John Yee of the University of California for **NASA's Jet Propulsion Laboratory**. *Further information is contained in a TSP [see page 1].*

NPO-20599

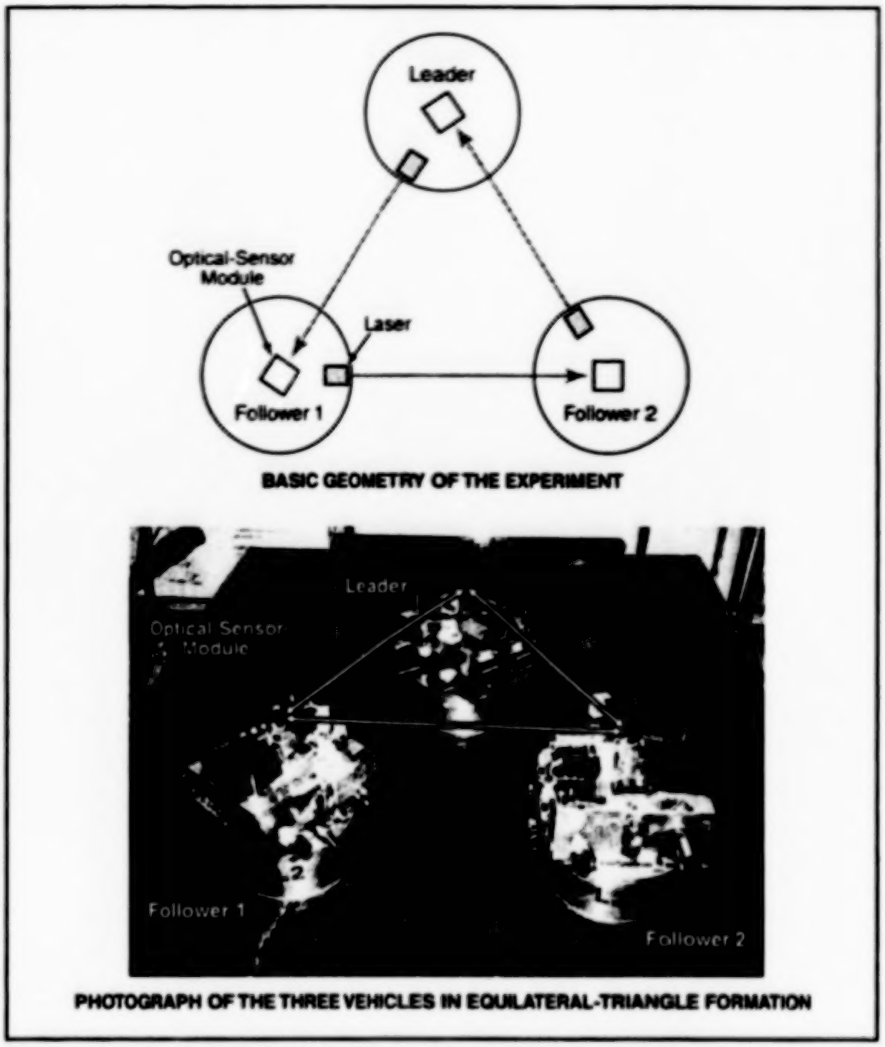

Three Autonomous Vehicles levitated on air bearings and propelled horizontally by air jets locate each other optically and align themselves in an equilateral triangle.

Pressure-Application Device for Testing Pressure Sensors

This device generates a pulse of known pressure.

Stennis Space Center, Mississippi

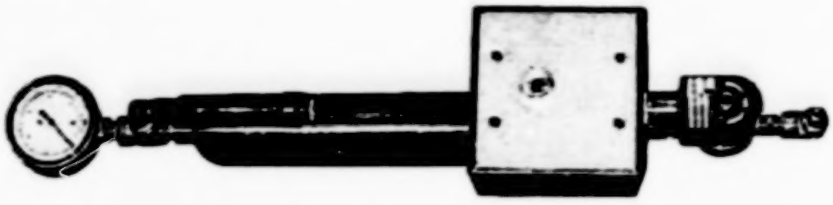

Air Is Manually Pumped into a cylinder for storage at a specified pressure. To test a pressure transducer, one presses a pushbutton to activate a solenoid valve that releases a pulse of pressurized air from the cylinder.

A portable pressure-application device has been designed and built for use in testing and calibrating piezoelectric pressure transducers in the field. The device generates pressure pulses of known amplitude. A pressure pulse (in contradistinction to a steady pressure) is needed because in the presence of a steady pressure, the electrical output of a piezoelectric pressure transducer decays rapidly with time.

The device (see figure) includes a stainless-steel compressed-air-storage cylinder of 500-cm^3 volume. A manual hand pump with check valves and a pressure gauge are located at one end of the cylinder. A three-way solenoid valve that controls the release of pressurized air is located at the other end of the cylinder. Power for the device is provided by a 3.7-V cordless-telephone battery. The valve is controlled by means of a pushbutton switch, which activates a 5-V to ±15-V DC-to-DC converter that powers the solenoid.

The outlet of the solenoid valve is connected to the pressure transducer to be tested. Before the solenoid is energized, the transducer to be tested is at atmospheric pressure. When the solenoid is actuated by the push button, pressurized air from inside the cylinder is applied to the transducer. Once the pushbutton is released, the cylinder pressure is removed from the transducer and the pressurized air applied to the transducer is vented, bringing the transducer back to atmospheric pressure. Before this device was used for actual calibration, its accuracy was checked with a NIST (National Institute of Standards and Technology) traceable calibrator and commercially calibrated pressure transducers.

This work was done by Wanda Solano of **Stennis Space Center** *and Greg Richardson of Lockheed Martin Corp.*

Inquiries concerning rights for the commercial use of this invention should be addressed to the Intellectual Property Manager, Stennis Space Center [see page 1]. Refer to SSC-00142.

Cylindrical Shape-Memory Rotary/Linear Actuator

A shape-memory ribbon is wrapped around a cylinder to build up length.

Lyndon B. Johnson Space Center, Houston, Texas

A compact actuator generates rotary or linear motion with a large torque or force, respectively. The original version of this actuator is designed to pull a wedge that, until pulled, prevents retraction of the proposed extended nose landing gear of the space shuttle. The original version is also required to fit into a volume that is severely limited by the size of the landing-gear assembly. The basic actuator design could be adapted to other applications in which there are requirements for compact, large-force actuators with similar geometries.

The transducer portion of this actuator is a ribbon of a nickel/titanium shape-memory alloy. A component made of such an alloy undergoes a pronounced deformation to a "remembered" shape (in the present case, the ribbon becomes shorter) when its temperature rises through a transition value, causing a transformation in its metallurgical structure from a martensitic phase to an austenitic phase. The component resumes its previous shape (in the present case, the ribbon lengthens) when its temperature falls below a lower transition temperature (there is hysteresis in the transformation). In this case, the transition temperatures are somewhat above room temperature.

To obtain sufficient length in order to obtain sufficient stroke, the shape-memory ribbon is wrapped three times around a cylinder. One end of the ribbon is attached to the cylinder, the other to an object that does not move, relative to the axis of the cylinder. The ribbon is heated by passing an electrical current through it. When the temperature of the ribbon rises above the first transition temperature, the resultant shape-memory shrinkage exerts a torque, causing the cylinder to turn. In the original application, the rotary motion of the cylinder is converted to linear motion by use of ramps, attached to the cylinder, that roll along wheels. In a different application, the rotary motion of the cylinder could be the desired output.

The primary difficulty encountered in initial tests was that the sliding friction engendered by wrapping the ribbon three times around the cylinder was so large as to impair actuation. The friction was reduced to an acceptably low level by placing the ribbon on nonconductive roller assemblies to enable the ribbon to move around the cylinder by rolling instead of sliding.

This work was done by Bradley Files and James W. Akkerman of **Johnson Space Center**. *Further information is contained in a TSP [see page 1].*
MSC-23211

Microfabricated Flow Controllers and Pressure Regulators

Efforts are underway to develop microfabricated flow controllers and pressure regulators that contain as few discrete components as feasible and that are cheaper, more robust, and orders of magnitude smaller than are currently commercially available devices that have similar capabilities. The developmental devices are designed to interact with electronic sensing and control circuits that include microprocessors that, in turn, communicate with host computers of digital feedback control systems. An example of the prototype devices constructed thus far is a hybrid device that includes a flow sensor, a valve containing a TiNi-alloy microribbon shape-memory actuator, and a temperature sensor, with wire-bonded leads for connection to electronic circuits. Windows™-based software for interaction between host computers and the microprocessors associated with these devices has been written. Contemplated further development efforts would be devoted to advancing from the concept of a flow controller on a ceramic substrate to that of a flow controller on an assembly of two or more semiconductor chips. In principle, fabrication on a semiconductor chip could be accomplished without need to assemble discrete components.

This work was done by A. David Johnson of TiNi Alloy Co. for **Kennedy Space Center**.

In accordance with Public Law 96-517, the contractor has elected to retain title to this invention. Inquiries concerning rights for its commercial use should be addressed to

A. David Johnson, Ph.D.
TiNi Alloy Co.
1619 Neptune Dr
San Leandro, CA 94577
Tel. No.: (510) 483-9676
E-mail: david@tinialloy.com

Refer to KSC-12104, volume and number of this NASA Tech Briefs *issue, and the page number.*

Books and Reports

Synchronizing Attitudes and Maneuvers of Multiple Spacecraft

A report discusses the problem of controlling the maneuvers of multiple spacecraft flying in formation and, more specifically, making the entire formation rotate about a given axis and synchronizing the rotations of the individual spacecraft with the rotation of the formation. Such formation flying is contemplated for mission in which the spacecraft would serve as platforms for long-baseline-interferometer elements and the synchronized rotations would be needed for slewing of the interferometers. Starting from (1) a particle model of the dynamics of the spacecraft formation, (2) a rigid-body model of the spacecraft-attitude dynamics, and (3) an assumption that one spacecraft would serve as the reference for the positions and orientations of the other spacecraft, the report presents a mathematical derivation of control laws for formation flying in the absence of gravitation and disturbances. A simplified control law suitable for implementation is also derived. Results of a computer simulation for three spacecraft flying in a triangular formation are presented to show that the control laws are effective.

This work was done by Fred Y. Hadaegh and Kenneth Lau of Caltech and Paul K. C. Wang of the University of California for **NASA's Jet Propulsion Laboratory**. *To obtain a copy of the report, "Synchronized Formation Rotation and Attitude Control of Multiple Free-Flying Spacecraft," see TSP's [page 1].*
NPO-20569

Machinery

Hardware, Techniques, and Processes

Mesoscopic Winch for Precise Extension and Retraction

A cable could be drawn in submicron steps over a range of ≈1 m.

NASA's Jet Propulsion Laboratory, Pasadena, California

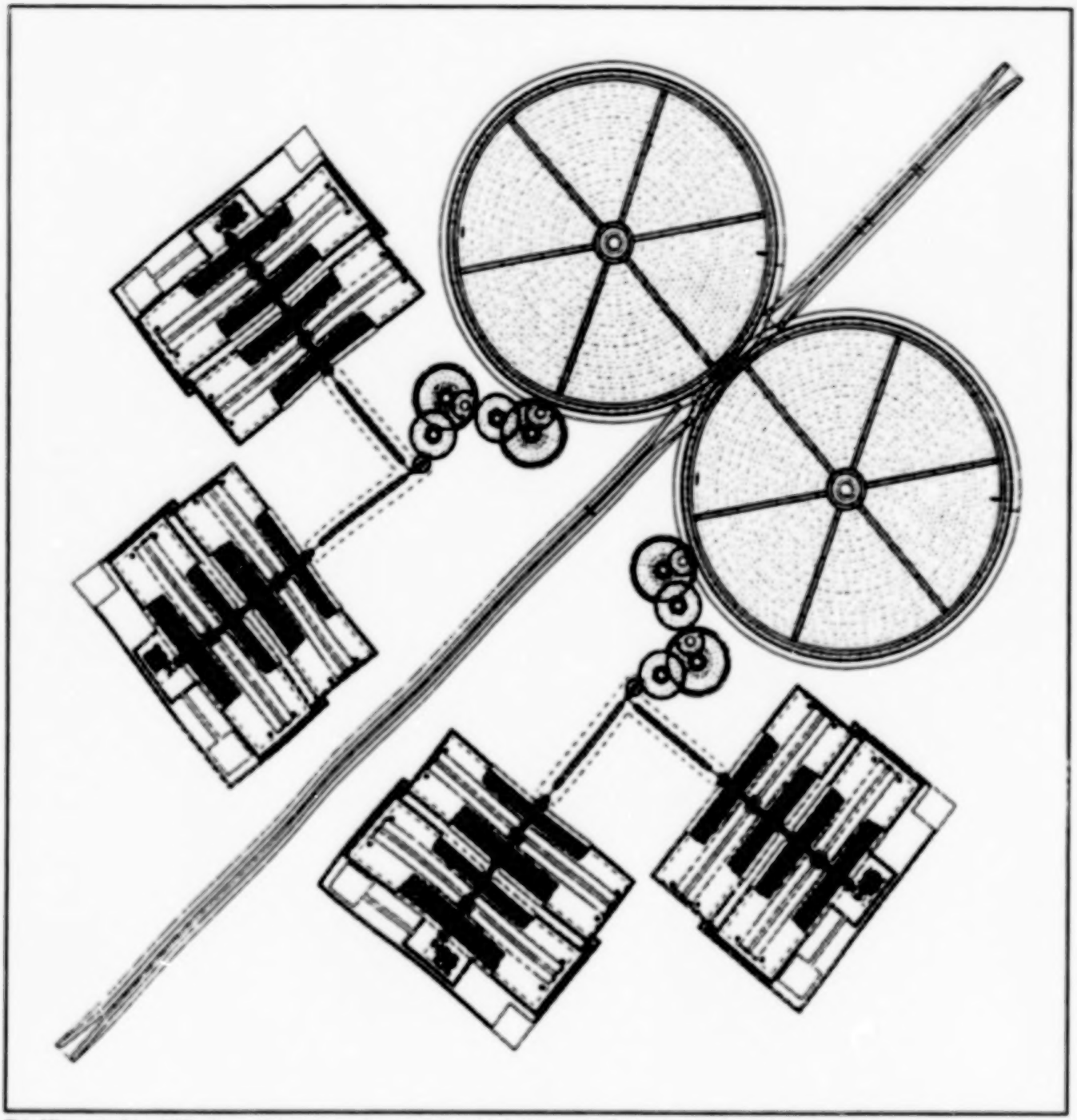

This Micromachined Winch would include comb actuators and reduction gears for retracting or extending a miniature cable.

A proposed lightweight, micromachined winch would have microscopic structural details and mesoscopic overall dimensions and would be capable of generating bidirectional macroscopic motion (maximum cable extension or retraction ≈1 m) with submicron increments. Winches like this one could be useful for actuating small mechanisms in scientific instruments and robots: examples of such mechanisms include translation stages; slide shutters and filters for imaging photodetector arrays; pan, tilt, or zoom actuators for cameras; mechanisms for dragging sampling scoops; and steering mechanisms for small robotic vehicles.

The proposed winch (see figure) would be fabricated in a four-layer polycrystalline-silicon surface-micromachining process. Electrostatic comb actuators would be the prime movers, generating motion in increments that gear trains would reduce to submicron values. The final gears in the gear trains would pinch and retract (or extend) a miniature cable, thereby generating the submicron increments of translation.

In one example design, the electrostatic

comb drives would operate in four-phase cycles. For each such cycle, a 19-tooth pinion gear would undergo one revolution. The pinion gear would be meshed with a 12.57-μm-pitch winch gear, so that one revolution of a pinion would result in a 238.8-μm translation. The thrust of each comb drive would be ≈1 μN and could be applied rapidly enough to sustain rotational speeds up about 4,000 revolutions per second. Two tandem gear trains would reduce the translation to 1.66 μm per pinion rotation or, equivalently, 0.415 μm per phase step of an electrostatic comb drive, and would increase the torque proportionally. Given the foregoing parameters, the maximum speed of retraction or extension of the cable would be ≈6 mm/s.

Assuming design rules and fabrication based on a fundamental design-rule length of 1 μm, the gear backlash per mesh would be ≈1 μm. For the purpose of precise positioning, it would be necessary to measure the aggregate backlash prior to operation and thereafter, during operation, correct for the aggregate backlash at each cable-drive reversal.

This work was done by Frank T. Hartley of Caltech for **NASA's Jet Propulsion Laboratory**. *Further information is contained in a TSP [see page 1].*
NPO-20979

Further Advances in Cooperative Transport by Mobile Robots

A gripping mechanism is presented for autonomous grasping/hoisting by two planetary rovers.

NASA's Jet Propulsion Laboratory, Pasadena, California

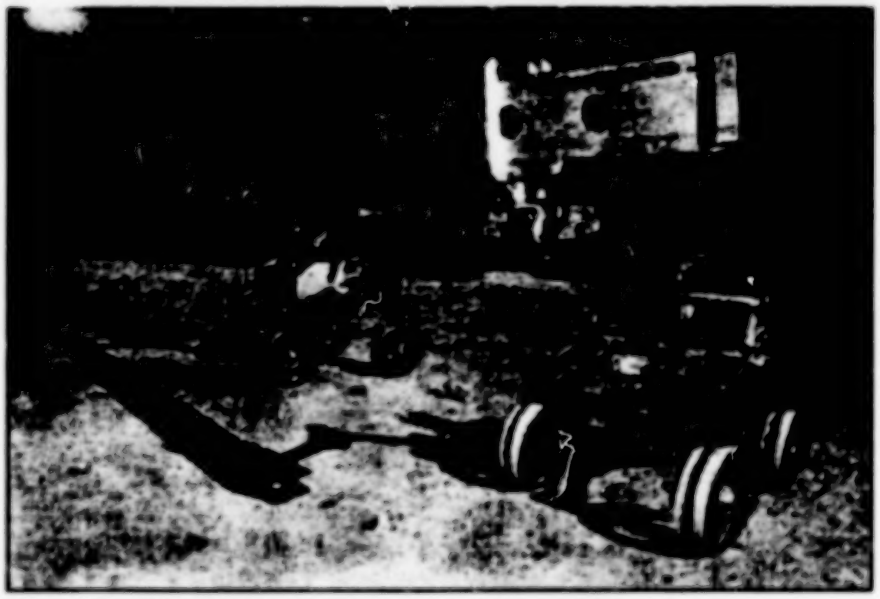

Figure 1. Two Mars Rovers cooperate in carrying a long payload.

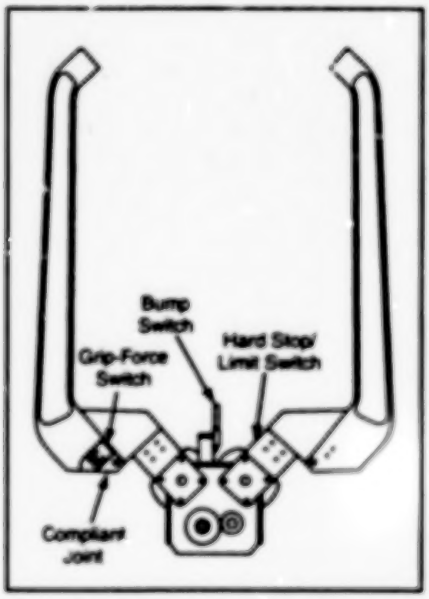

Figure 2. A Gripper includes two fingers that straddle and oppose a thumb. The fingers and thumb are connected at their bases to compliant pivots counterrotated by a motor and transmission.

Hardware and decentralized-control algorithms have been developed during continued research on the sensors, the actuators, and the design and functional requirements for systems of multiple mobile robots cooperating in the performance of tightly coupled tasks — for example, grasping and lifting long objects on challenging terrain. [Different aspects of the hardware and algorithms were described in "Advances in Cooperative Transport by Two Mobile Robots" (NPO-30376) *NASA Tech Briefs*, August 2002. Although this research is oriented toward developing robotic capabilities for exploration of Mars, these capabilities could also be utilized on Earth.

Two robots used in this research have been rovers designed for prototype Mars missions: the Sample Return Rover and the Sample Return Rover 2000 (see Figure 1). Robotic arms (manipulators) on both rovers were modified to include grippers redesigned as their end effectors. Each gripper (see Figure 2) is of a simple yet novel design, incorporating three interlocking digits: Two fingers facing one side straddle a thumb that faces the opposite side, and these opposing digits are driven at their respective bases by counterrotating, parallel pivots. The finger and thumb pivots are driven through a transmission actuated by a single DC motor equipped with an incremental-shaft-angle encoder for feedback. The fingers and thumb are hooked at their tips to provide positive retention against slippage of a grasped payload. The finger geometry accommodates a variety of payloads of any general cross section narrow enough to fit between the fingers.

The design of the grippers provides passive compliance to simplify control of the gripping process: A spring-loaded pivot at the base of each digit enables flexing to "open up the grip," when the payload exerts an overload on the gripper. In the absence of a payload, mechanical hard stops and limit switches arrest the gripper and signal its closure. The compliant joint on each digit also includes a switch that provides limited feedback related to the gripping force, by signaling the point at which each digit flexes open. Another sensor that provides feedback is located in the "palm" of the gripper: a compliant bumper on a switch provides information related to the location of the payload; that is, whether or not the payload has been grasped.

The cooperative grasping and lifting behavior of the robots is characterized as being partitioned into the following four distinct phases:

1. *Visual Target Search Phase*

In this phase, cameras on the rovers are used to search and capture images of unique patterns placed at specified posi-

tions on the payload. From the images, estimates of the Cartesian coordinates of the point of grasp and of an approach unit vector are computed for each rover. Estimates of the distance each rover must travel and the orientation that each rover must assume to place the payload within the work space of its manipulator are also computed. Synchronization occurs between the rovers, and both rovers proceed to position and orient themselves within their respective manipulator work spaces. The rovers then proceed to the approach phase.

2. *Approach Phase*

The gripper of each rover is moved along the approach unit vector toward the point of grasp computed during the visual target search phase, until the palm contact switch is triggered. If contact is made as indicated by the thumb or finger switch during the approach, the gripper is moved away from the payload until thumb or finger switch is reset and the approach phase aborted. This completes the approach phase. Synchronization occurs between the rovers before proceeding to the grasp phase.

3. *Grasp Phase*

The digits are moved in such a manner as to ensure that the finger and thumb contact switches are triggered, confirming a firm grip of the payload. The gripper is not equipped with force and torque sensors; instead, the spring preloads of compliant joints are adjusted manually ahead of time to set the approximate value of the gripping force or a prescribed amount of overtravel is used to give an estimated gripping force.

An "intelligent" heuristic, rule-based compliance-control algorithm is implemented by use of the limited feedback provided by the contact switches during grasping. If the thumb contact switch is closed independently of any finger contact switch, the arm is moved perpendicular to approach unit vector until the thumb contact switch is reset to the open condition. A similar maneuver is performed if either or both of the finger contact switches are triggered independently of the thumb contact switch. These compensatory maneuvers have been demonstrated to guarantee a firm grasp with rover positioning errors of as much as 5 cm.

4. *Payload Lift Phase*

In this phase, the payload is lifted about 20 cm in two stages: 5 cm in the first stage and 15 cm in the second stage.

It is easy to develop control algorithms that use the information provided by the switches on the fingers and thumb, along with the information from the bump switch in the palm, to deduce whether the payload is within grasp; that help to center the gripper about the payload; and that deduce minimal information about the orientation of the payload. For example, by determining which finger is flexing, such an algorithm can help to determine the angle of the payload.

This work was done by Ashitey Trebi-Ollennu, Hari Das Nayar, and Anthony Ganino of Caltech for **NASA's Jet Propulsion Laboratory**. *Further information is contained in a TSP [see page 1].*

NPO-30511

BLANK PAGE

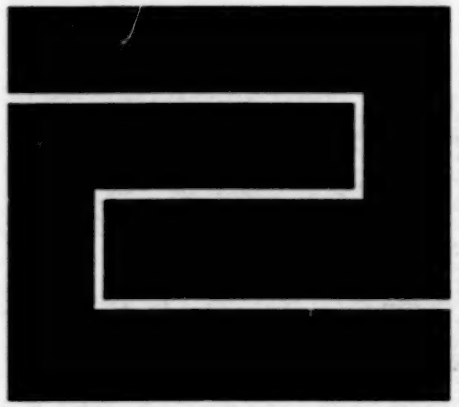

Fabrication Technology

Hardware, Techniques, and Processes

BLANK PAGE

Low-Temperature Thermocompressive Au-to-Au Diffusion Bonding

This technique is suitable for fabrication of microelectromechanical structures.

NASA's Jet Propulsion Laboratory, Pasadena, California

A technique of thermocompressive gold-to-gold diffusion bonding at relatively low temperature has been devised to provide stable, uniform, strong bonds between structural components of microelectromechanical systems. The technique can also be used for vacuum sealing of microscopic cavities. Unlike some other metal-to-metal diffusion bonding techniques, this technique does not entail significant outgassing or the formation of intermetallic compounds. The technique is suitable for bonding of parts made of silicon, quartz, low-thermal-expansion glass, and other materials that can withstand the relatively mild rigors of a low-temperature thermocompressive-bonding process.

Two parts to be joined by this technique must have faying surfaces that are either flat or shaped to fit each other. In preparation for bonding, each of the faying surfaces is coated with a layer of chromium, then with a layer of gold (see figure). The coating is done by electron-beam evaporation. The coated substrates are cleaned, then clamped together with their gold layers touching in the desired final configuration in a press in a vacuum chamber.

The chamber is evacuated to a pressure of about 10^{-5} torr (about 1.3×10^{-3} Pa). While maintaining the clamping force and the vacuum, the coated parts are heated to a temperature in the approximate range of 100 to 350 °C for about 1 hour. The combination of heating and clamping pressure in the vacuum causes atoms to diffuse and mix between the touching gold layers of the two parts, forming a single gold layer that bonds the two parts together.

This work was done by Tony K. Tang and Roman Gutierrez of Caltech for **NASA's Jet Propulsion Laboratory**. *Further information is contained in a TSP [see page 1].*

This invention is owned by NASA, and a patent application has been filed. Inquiries concerning nonexclusive or exclusive license for its commercial development should be addressed to the Patent Counsel, NASA Management Office–JPL [see page 1]. Refer to NPO-20076.

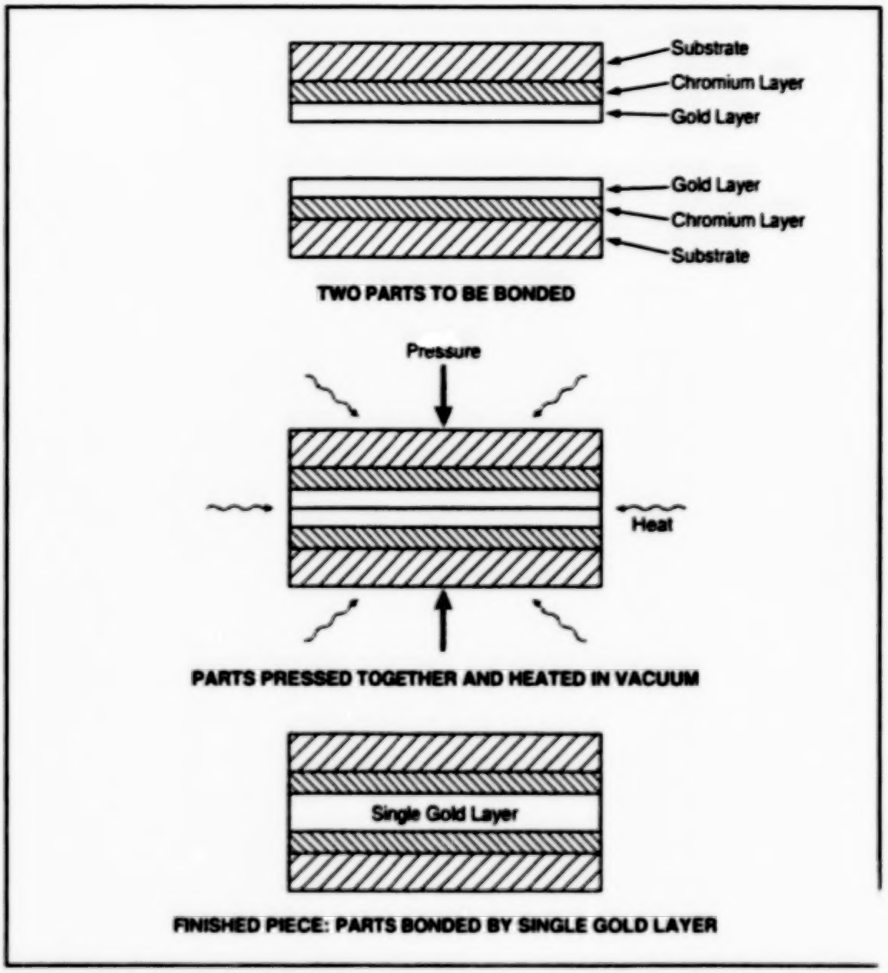

The Two Parts Are Pressed Together and heated in a vacuum, causing diffusion and mixing of gold atoms. As a result, the two gold layers become one.

Growing Carbon Nanotubes Aligned With Patterns

Positions and orientations of individual nanotubes could be tailored.

NASA's Jet Propulsion Laboratory, Pasadena, California

A process has been proposed for growing carbon nanotubes aligned substantially parallel with the nominal planar surfaces of substrates and further aligned with patterns on the substrates. Prior to growth, the patterns would be formed by micromachining the substrates, which could be silicon or silicon-on-insulator (SOI) wafers. By making it possible to tailor the positions and orientations of individual carbon nanotubes grown on pre-patterned substrates, this process would enable advances in nanotube-based electronic and electromechanical devices.

The process would include chemical vapor deposition (CVD) of the carbon nanotubes on patterned catalysts on the substrates. In each case, the CVD gas would consist of a source of carbon (such as methane, ethylene, or carbon monoxide) either by itself or in a mixture with other gases. Carbon nanotubes grow when a substrate with patterned catalyst is heated and exposed to this CVD gas mixture under appropriate conditions [which can include enhancement by RF (radio frequency) plasmas and/or hot filaments].

The basic process admits of three main variants, each involving a different technique or combination of techniques to position and orient the growing carbon nanotubes.

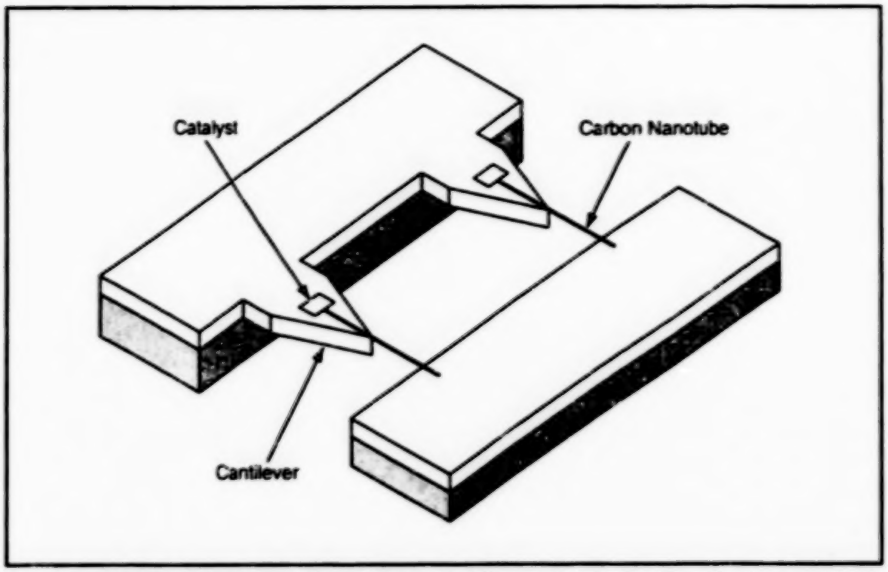

Figure 1. **Carbon Nanotubes Would Grow in Alignment** with the tips of micromachined cantilevers on an SOI wafer.

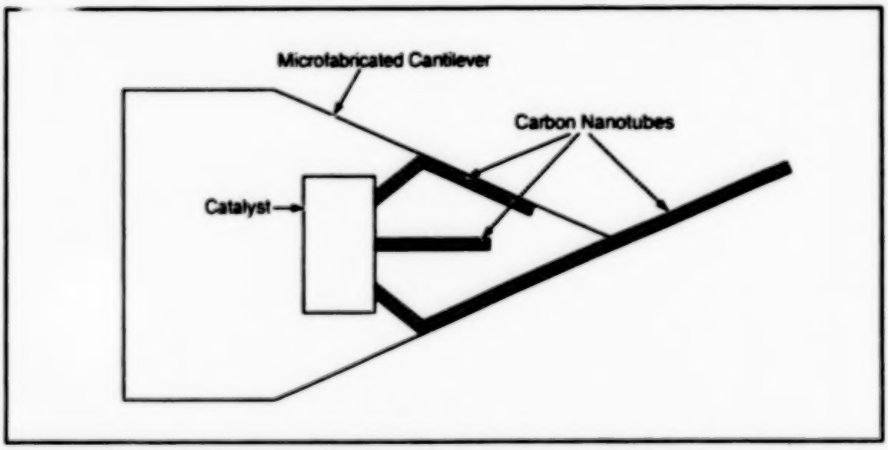

Figure 2. **Nanotubes Would Tend To Grow Along Surfaces and Edges** because of van der Waals attraction, but could not follow sharp bends. The growing nanotubes tubes would therefore be expected to grow toward the sharp tip of the cantilever. One of the growing nanotubes could be expected to end up protruding from the tip in a predetermined direction.

In the first variant (the basic process), the desired alignment would be enforced by use of in-plane pointed silicon cantilevers protruding from an undercut silicon layer on an SOI substrate (see Figure 1). Part of the upper surface of each cantilever would be coated with a thin film of a suitable catalyst (e.g., Ni, Co, or a suitable metal alloy or compound).

On the basis of prior experiments on the growth of nanotubes, it is expected that (1) the nanotubes will tend to nucleate at random times and locations, such that multiple tubes may grow out of each catalyst film, and (2) because of attractive van der Waals forces, the nanotubes will tend to grow along the cantilever surfaces and edges. It is also anticipated that if the tip of a growing nanotube reaches the tip of the cantilever, further growth would likely cause the nanotube to protrude from the tip because strain-energy cost of bending the nanotube to the small tip radius would exceed the energy of van der Waals attraction (see Figure 2).

In the second variant of the process, the micromachined patterns would comprise narrow, etched trenches in silicon wafers. Enhanced van der Waals forces at the edges of the trenches would preferentially align the growing nanotubes.

In the third variant of the process, electric fields would be used to align the growing nanotubes. In this case, each substrate would be prepared by microfabrication of (1) pointed cantilevers similar to those of the first variant of the process and (2) on-chip electrodes. A bias potential applied during growth would result in a high local electric field between an electrode on the tip of each cantilever and a nearby electrode. The bias circuitry would be designed to prevent the large surges of current that would destroy the growing nanotubes as the interelectrode gaps became bridged by growth of the nanotubes (e.g., by incorporating a large series resistor in the circuit). It may be necessary to adjust the pressure of the CVD gas and/or electrode spacing to prevent electrical discharges between the biased electrodes.

This work was done by Brian Hunt, Daniel Choi, Michael Hoenk, Robert Kowalczyk, and Flavio Noca of Caltech for **NASA's Jet Propulsion Laboratory.** *Further information is contained in a TSP [see page 1].*

In accordance with Public Law 96-517, the contractor has elected to retain title to this invention. Inquiries concerning rights for its commercial use should be addressed to

Intellectual Property group
JPL
Mail Stop 202-233
4800 Oak Grove Drive
Pasadena, CA 91109
(818) 354-2240

Refer to NPO-30205, volume and number of this NASA Tech Briefs *issue, and the page number.*

Process for Rapid Prototyping in Ceramic-Matrix Composites

Precursors of continuous-fiber-reinforced CMCs are deposited in patterned layers.

Marshall Space Flight Center, Alabama

The ceramic-composite advanced tow-placement (CCATP) process is a means of laying down continuous-fiber-reinforced, ceramic-matrix composite (CMC) materials in patterned layers to form objects that could have complex three-dimensional shapes. The CCATP process is a member of the growing family of solid-freeform processes in art of rapid prototyping.

In preparation for CCATP, tows of fibers (of which the main ingredients are typically graphite or silicon carbide) are first coated with an interfacial material (e.g., pyrolytic graphite or boron nitride) to prevent damage in subsequent processing. The fibers

are then coated with a mixture of a ceramic matrix material in powder form plus a thermoplastic or other low-temperature binder. The resulting tows of coated fibers are wound on spools.

The CCATP process is effected by use of advanced tow-placement (ATP) equipment that includes, among other things, a robotic head that is moved to deposit the tows in the specified patterned layers. As the robotic head moves, the tows are paid out from the spools, heated, and pressed onto the surface of the object to be formed. The process parameters and the motion of the robotic head can be controlled by use of output data from a computer-aided design (CAD) system.

The head includes two rollers and two hot-nitrogen-gas torches that heat the rollers and the deposited material. The first torch and roller preheat both the incoming material and the previously deposited material or substrate. The first roller serves further to press and thereby tack the incoming material onto the previously deposited material or substrate. The second torch provides through-the-thickness heating to facilitate both consolidation of the just-deposited tow material and further bonding (beyond mere tacking) of the just-deposited tow material to the previously deposited material. The second roller completes the consolidation and bonding by pressing the just-deposited and previously deposited material together with enough force to prevent the formation of voids in the material.

A workpiece can be formed to nearly the desired net size and shape in the CCATP process. The size and shape can include allowances for small changes that occur in the next processing step, in which the workpiece is heated to burn out the binder and sinter the ceramic matrix to complete the synthesis of the composite material.

This work was done by Michael R. Effinger of **Marshall Space Flight Center**, *Ranji K. Vaidyanathan, Mark Fox, Mark J. Rigali, and Anthony C. Mulligan of Advanced Ceramics Research, Inc.; and John W. Gillespie, Jr. and Shridhar Yarlagadda of The Center for Composite Materials, University of Delaware. For further information, contact the company at (520) 573-6300 or see TSP's [page 1]*

In accordance with Public Law 96-517, the contractor has elected to retain title to this invention. Inquiries concerning rights for its commercial use should be addressed to

Advanced Ceramics Research, Inc.
3292 E. Hemisphere Loop
Tucson, AZ 85706

Refer to MFS-31597, volume and number of this NASA Tech Briefs *issue, and the page number.*

BLANK PAGE

Mathematics and Information Sciences

Hardware, Techniques, and Processes

Initialized Fractional Calculus

Initialization functions are essential to a revised formulation suitable for engineering and scientific applications.

John H. Glenn Research Center, Cleveland, Ohio

The fractional calculus (which admits of integrals and derivatives of non-integer order) dates back almost to the origin of the better-known ordinary (integer-order) calculus, but thus far has been treated more as a mathematical curiosity than as a scientific and engineering tool. Increasingly many physical processes are found to be best described using fractional differential equations. These processes include: viscoelasticity, rheology, electrochemistry, fractal processes, and many diffusion processes. The application of the fractional calculus to scientific and engineering problems has been inhibited by difficulties that arise from the basic definitions given heretofore for integrals and derivatives of arbitrary order. These difficulties are associated with the initialization problem, which is explained below.

Consider a function $f(t)$, where t could be time or any other independent variable, and let ${}_cD_t^v f(t)$ denote the vth-order derivative of f with respect to t (where v is a positive real number and not necessarily a integer). One of the properties that must be preserved to make the fractional calculus compatible with the ordinary calculus is the composition or the index law, which is represented by the following equation:

$${}_cD_t^u\,{}_cD_t^v f(t) = {}_cD_t^v\,{}_cD_t^u f(t) = {}_cD_t^{u+v} f(t).$$

The initialization problem arises as follows: One of the requirements of prior formulations of the fractional calculus is that in order to preserve composition, $f(t)$ and all of its derivatives must be identically zero at $t = c$. Inasmuch as it is difficult to make all functions and derivatives of interest initially zero in many scientific and engineering problems, this requirement has effectively rendered until now the fractional calculus inapplicable in such cases.

As its name suggests, the initialized fractional calculus is formulated to address the initialization problem. In the initialized fractional calculus, it is not required that $f(t)$ and its derivatives be zero at $t = c$ in order to preserve composition. What enables the elimination of this requirement is the revision of definitions of integrals and derivatives of arbitrary orders to include initialization functions that carry the history of the differintegral. The initialization functions are generalizations of the constants of integration that appear in the ordinary calculus, where they are used to represent initial conditions.

Other major topics addressed in the development of the initialized fractional calculus include the following:

- Heretofore, Laplace transforms have been the primary tools for solving fractional differential equations. Therefore, the basic Laplace transforms for the initialized fractional integrals and derivatives were developed.
- The concept of a variable-structure or variable-order differintegral was introduced. This concept can be represented by the fractional differential equation ${}_cD_t^{q(t)} y(t) = f(t)$ and the companion inferred integral equation ${}_cD_t^{-q(t)} f(t) = y(t)$, where q (the structure or order parameter) is a function of t or y. Some phenomena in viscoelasticity and diffusion appear to be amenable to treatment by fractional differential equations with variable order parameters.

Going beyond viscoelasticity, the initialized fractional calculus can be applied to problems that arise in a variety of scientific, engineering, and purely mathematical disciplines, including creep, percolation, material science, viscous fluid behavior, heat transfer, batteries, electromagnetics, control, communications, filtering, and chaotic systems.

This work was done by Carl F. Lorenzo of **Glenn Research Center** *and Tom T. Hartley of the University of Akron. Further information is contained in a TSP [see page 1].*

Inquiries concerning rights for the commercial use of this invention should be addressed to NASA Glenn Research Center, Commercial Technology Office, Attn: Steve Fedor, Mail Stop 4–8, 21000 Brookpark Road, Cleveland, Ohio 44135. Refer to LEW-17139.

Algorithm Plans Motion of Robot With Limited Field of View

The RoverBug algorithm plans the motion of a robotic vehicle (rover) equipped with a CCD (charge-coupled device) camera or comparable sensor that has a limited field of view. The algorithm produces locally optimal (shortest-distance) paths across unbounded, previously unknown terrain; utilizes gaze control to minimize the amount of sensing; and avoids unnecessary robot motion. Because this algorithm is based on a local and simple mathematical model of terrain, it does not entail the bookkeeping of a global model (with all of the attendant issues of registration of local maps with global ones and with each other), and does not require the large memory that would be required by a global model. The algorithm is amenable to varying levels of autonomy, ranging from single-subpath execution under tight operator guidance to completely autonomous traverses to distant goals. In addition to being useful for exploration of distant planets via rovers, the algorithm could be applied in such terrestrial scenarios as cleanup of environmental hazards or military surveillance. A version of the algorithm has been implemented on NASA's Rocky 7 prototype microrover.

This work was done by Sharon Laubach of Caltech for **NASA's Jet Propulsion Laboratory**. *Further information is contained in a TSP [see page 1].*

This software is available for commercial licensing. Please contact Don Hart of the California Institute of Technology at (818) 393-3425. Refer to NPO-30241.

Product Attributes Database

Product Attributes Database (PAD) is a computer program that enables a team of engineers, managers, and administrators involved in a product-development project to collaborate more effectively. PAD serves as a single, network-accessible repository for all essential parametric information (the database) that characterizes the project at any phase of implementation. PAD collects and organizes the data into a human-readable format so that any member of the team can gain access to the data and/or link the data to documents, reports, and presentations. The PAD information architecture includes interfaces to several soft-

ware systems, including programs for engineering design and analysis, estimation of costs, testing and verification of designs, documentation, and display of data. These interfaces support real-time, collaborative engineering. Going beyond prior engineering-database programs, PAD includes both (1) a machine-interface subsystem that enables a variety of engineering and administrative programs to work together through the database over a network and (2) a human-interface subsystem, which provides a simple graphical user interface that enables a team member to read and write data from any network-accessible computer.

This work was done by Thomas Clymer, William Heinrichs, and Joel Sercel of Caltech for **NASA's Jet Propulsion Laboratory**. *Further information is contained in a TSP [see page 1].*

This software is available for commercial licensing. Please contact Don Hart of the California Institute of Technology at (818) 393-3425. Refer to NPO-20673.

Flash Automated Updating of Software in Multiple Computers

Program and data files in the Unified Control Modules (UCMs) of the Operational Television system at Kennedy Space Center are updated rapidly and automatically in a scheme that exploits unique features of the UCM design. Each UCM includes a VersaModule Eurocard (VME) chassis, in which are installed several single-board central processing units (CPUs) and a board that holds 8MB of flash electrically erasable, programmable read-only memory that is accessible to all the CPUs via the VMEbus. This flash memory can be erased and reprogrammed without removing the memory circuitry from the UCM. The CPUs utilize the VxWorks real-time operating system, which provides, among other things, interprocessor communication via the VME backplane, support for networking, and support for MS-DOS file systems. A VxWorks driver program creates an MS-DOS file system in the flash memory and provides for access to, and manipulation of, the files. Each time the UCM is rebooted, one CPU, designated the main CPU first determines whether a designated host computer is available in a network to which the UCM is connected. If so, the main CPU obtains a list, stored in the host computer, of files that should be in the flash memory. If it finds that the modification date and time of a given file in the host differs from those in the flash memory or if the file does not exist in flash memory, then the file is copied to the flash memory. Once flash-memory files have been thus updated, the main CPU signals the other CPUs to complete their booting and gain access to the files in the flash memory card via the VMEbus.

This work was done by Charles H. Chapman of Dynacs Engineering Co., Inc., for **Kennedy Space Center**. *Further information is contained in a TSP [see page 1].*
KSC-12120

END

10-27-04